Novel (Cyanamide)Zn^{II} Complexes and Zinc(II)-mediated Hydration of the Cyanamide Ligands

Andrey S. Smirnov,[a] Ekaterina S. Butukhanova,[a] Nadezhda A. Bokach,*[,a] Galina L. Starova,[a] Vladislav V. Gurzhiy,[a] Maxim L. Kuznetsov[b] and Vadim Yu. Kukushkin*[,a]

[a] Institute of Chemistry, Saint Petersburg State University, Universitetsky Pr. 26, 198504 Stary Petergof, Russian Federation

[b] Centro de Química Estrutural, Complexo I, Instituto Superior Técnico, Universidade de Lisboa, Avenida Rovisco Pais, 1049-001 Lisbon, Portugal

Abstract

The cyanamides $NCNR_2$ (R_2 = Me_2, Ph_2, C_5H_{10}) react with ZnX_2 (X = Cl, Br, I) in a 2:1 molar ratio at RT giving a family of the zinc(II) complexes $[ZnX_2(NCNR_2)_2]$ (R_2 = Me_2, X = Cl **1**, X = Br **2**, X = I **3**; R_2 = C_5H_{10}, X = Cl **4**, X = Br **5**; X = I **6**; R_2 = Ph_2, X = Cl **7**, X = Br **8**, X = I **9**; 75–92% yields). Complexes **7** and **8** undergo ligand redistribution in wet CH_2Cl_2 solutions giving the $[Zn(NCNPh_2)_4(H_2O)_2][Zn_2(\mu-X)_2X_4]$ (X = Cl **10**, Br **11**) species that were characterized by ^{1}H NMR, HRESI-MS, and X-ray diffraction. Halide abstraction from **1–3** by action of $AgCF_3SO_3$ or treatment of $Zn(CF_3SO_3)_2$ with $NCNR_2$ (R_2 = Me_2, C_5H_{10}) lead to labile complexes $[Zn(CF_3SO_3)_2(NCNR_2)_3]$ (R_2 = Me_2, **12**; C_5H_{10}, **13**). Crystallization of **12** from wet CH_2Cl_2 or from the reaction mixture gave $[Zn(NCNMe_2)_3(H_2O)_2](SO_3CF_3)_2$ (**12a**) or $[Zn(CF_3SO_3)_2(NCNMe_2)_2]_\infty$ (**12b**), whose structures were determined by X-ray diffraction. The Zn^{II}-mediated hydration was observed for the systems comprised of ZnX_2 (X = Cl, Br, I), 2 equiv $NCNR_2$ (R_2 = Me_2, C_5H_{10}, Ph_2) and *ca.* 40-fold excess of water and conducted in acetone at

60 °C ($R_2 = Me_2$, C_5H_{10}) or 80 °C ($R_2 = Ph_2$) in closed vials and it gives the urea complexes

[ZnX_2{$OC(NR_2)NH_2$}] ($R_2 = Me_2$, X = Cl **13**, X = Br **14**, X = I **15**; R = C_5H_{10}, X = Cl **16**, X = Br

17; X = I **18**; $R_2 = Ph_2$, X = Cl **19**, X = Br **20**, X = I **21**; 57–81%). In contrast to the Zn^{II}-

mediated hydration of conventional nitriles, that proceeds only in the presence of co-catalyzing

oximes or carboxamides, the reaction with cyanamides does not require any co-catalyst.

Complexes **1**–**9**, **12**–**19**, were characterized by ^{1}H, ^{13}C{^{1}H} NMR, IR, HRESI-MS, and X-ray

crystallography (for **1**–**3**, **8**, **9**, **13**–**15**, and **17**), whereas **20** and **21** were characterized by

HRESI$^+$-MS and ^{1}H and ^{13}C{^{1}H} NMR (for **20**). The structural features of the cyanamide

complexes **1**, **2**, **7**, and **8** were interpreted by theoretical calculations at DFT level.

Introduction

The conversions of nitrile substrates are among the most significant processes for both

laboratory and industry. Typically, reactions of NCR species require an additional activation of

the C≡N group, in particular, by its ligation to a metal center. Various reactions of metal-

acivated NCR's were intensively investigated for the past two decades and this topic was

repeatedly surveyed along the years[1–11] including our reviews in this field.[1,3,8] In contrast, the

chemistry of cyanamides $NCNR_2$ (R = alkyl, aryl) is incomparably less investigated, although

some works on their coordination chemistry prove that $NCNR_2$ ligands exhibit excitingly

different behavior at the *quantitative*- and at the *qualitative* levels as compared to the

conventional nitriles NCR (R = alkyl, aryl).[12–20] In recent works, we studied reactivity of nitrile

and cyanamide ligands at platinum(II- and IV) and palladium(II) centers and observed

significant differences in reaction rates and also in the nature of products derived from metal-

mediated conversion of dialkylcyanamide and conventional nitrile ligands.[12–20]

In the current work, we focused our attention on cyanamide metal systems bearing much

more kinetically labile metal center than platinum or palladium, viz. zinc(II). The cyanamide

zinc chemistry is almost unexplored and, to the best of our knowledge, there is only one report

describing the two (cyanamide)Zn^{II} compounds[12,21] [ZnCl$_2$(NCNiPr$_2$)$_2$] and [ZnCl$_2$(NCNiPr$_2$)(H$_2$O)]. Moreover, no data on activation of cyanamide substrates by zinc centers were so far reported.

The goals of this work were at least two-fold: (*i*) to develop a general synthetic route to a new family of (cyanamide)Zn^{II} complexes and to study structural features of these species and their conversions in solutions, (*ii*) to investigate reactivity of cyanamide substrates at zinc(II) centers toward nucleophilic addition, *e.g.* hydration, providing the comparison of their reactivity with that observed for conventional nitrile ligands.

Results and Discussion

Synthesis and characterization of [ZnX$_2$(NCNR$_2$)$_2$]. Preliminary specific conductivity and HRESI-MS tests were performed for the ZnX$_2$/NCNR$_2$ (X = Cl, Br, I; R$_2$ = Me$_2$, C$_5$H$_{10}$, Ph$_2$; 0.02 mmol of ZnX$_2$ and 0.04 mmol of NCNR$_2$ – in all possible combinations) systems in CH$_2$Cl$_2$ (10 mL) at RT. The progress of these reactions was monitored for the period from 1 min to 48 h after mixing the reagents and the most significant changes were observed for the first 5 h. After 48 h specific conductivity increased from ca. 0.00 to 0.96–3.17, 0.73–0.82, and 0.95–1.28 μS•cm^{-1} for X = Cl, Br, and I, respectively. However, the final values still closer to marginal conductivities of non-electrolyte type compounds.

Immediately after mixing the reactants, the ions [Zn + X + 2NCNR$_2$]$^+$, [Zn + X + NCNR$_2$]$^+$ (for all systems) and, in addition, [Zn + I + 3NCNR$_2$]$^+$ (for X = I; R$_2$ = C$_5$H$_{10}$, Ph$_2$) were detected in HRESI$^+$-MS, whereas the [ZnX$_3$]$^-$, [Zn$_2$X$_5$]$^-$ ions were observed in HRESI$^-$-MS. When the reaction mixtures were kept for 5 h, the peaks from [Zn + X + 3NCNR$_2$]$^+$ were detected by HRESI$^+$-MS for all mixtures, besides the X = I, R$_2$ = Me$_2$ system, and the ions with higher degrees of oligomerization, viz. [Zn$_3$X$_7$]$^-$, [Zn$_4$X$_9$]$^-$, [Zn$_5$X$_{11}$]$^-$, were found in the HRESI$^-$-MS (X = Cl, Br). For the ZnI$_2$/NCNC$_5$H$_{10}$ system, the [Zn$_2$I$_3$(NCNC$_5$H$_{10}$)$_3$]$^+$ ion was also observed although intensity of its peaks was rather small even after 5–7 h. All other signals,

which were detected by HRESI right after mixing, also displayed in the mass-spectra after 7 h. One should notice that the $[Zn(NCNPh_2)_4]^{2+}$ ion was detected in HRESI$^+$-MS of $ZnCl_2$/NCNPh$_2$ system, derived from more concentrated solution (0.1 mol/L $ZnCl_2$), even after 5 min and the appropriate set of peaks became the most intensive after 10 d.

In synthetic experiments, the complexes $[ZnX_2(NCNR_2)_2]$ (R$_2$ = Me$_2$, X = Cl **1**, X = Br **2**, X = I **3**; R$_2$ = C$_5$H$_{10}$, X = Cl **4**, X = Br **5**; X = I **6**; R$_2$ = Ph$_2$, X = Cl **7**, X = Br **8**, X = I **9**) were prepared by treatment of ZnX_2 with two equivs of the corresponding cyanamide in dry dichloromethane at RT for 2 h (**Scheme 1**). Under these conditions we succeeded in the isolation of the pure $[ZnX_2(cyanamide)_2]$ (**1–9**) complexes as rather hygroscopic colorless solids obtained in 75–92% yields.
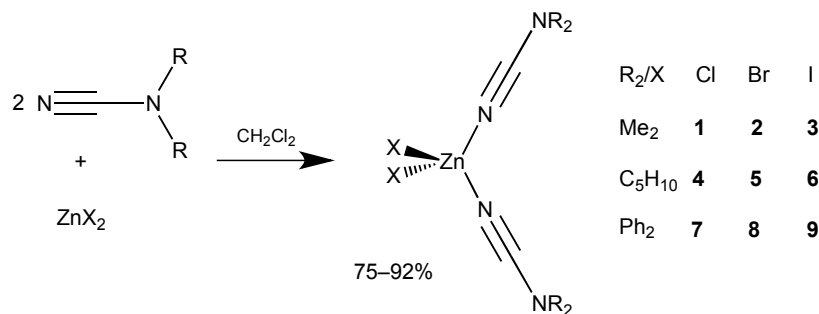
Scheme 1. Synthesis and numbering of $[ZnX_2(NCNR_2)_2]$.

Previously only one representative of this dichloro*bis*(cyanamide) family, *viz.* $[ZnCl_2(NCN\textit{i}Pr)_2]$, was obtained by treatment of $ZnCl_2$ with two equivs of diisopropylcyanamide in dichloromethane solution and this complex was characterized by IR, NMR, and elemental analyses; no X-ray structural data were obtained.[21] One should also notice that complexes $[ZnCl_2(NCR)_2]$ bearing conventional nitrile ligands, in contrast to their cyanamide analogs, are substantially more abundant.[22–31]

Despite metal complexes featuring NCN(H)Ph species are rather common and their chemistry has been reviewed,[32] the coordination chemistry of its diphenyl congener, NCNPh$_2$, is almost unexplored and only one example of the NCNPh$_2$ Lewis acid complex,

4

[SbCl$_5$(NCNPh$_2$)], was reported.[21] As far as the application of NCNPh$_2$ in organometallic chemistry is concerned, diphenylcyanamide, similarly to the other *bis*-substituted cyanamides NCNR$_2$ (R = Me, Et, Pr, *i*-Pr), reacts with the carbene complexes [M(CO)$_5${C(Ph)R^1}] (M = Cr, W; R^1 = Ph, OMe) giving the insertion products [M(CO)$_5${C(NPh$_2$)N=C(Ph)R^1}].[33] Furthermore, alkylation of NCNPh$_2$ leads to a highly reactive nitrilium salt, which easily reacts with methanol.[21] Thus, we notice here that complexes **7**–**9** are the first representatives of transition metal species bearing NCNPh$_2$ ligands.

Zinc complexes **1**–**9** were characterized by elemental analysis for Zn and HRESI-MS, as well as IR, ^{1}H, ^{13}C{^{1}H}, and (for the triflate-containing species) ^{19}F{^{1}H} NMR spectroscopies. Five compounds, viz. **1**–**3**, **8**, and **9**, were studied by single-crystal X-ray diffraction. The HRESI$^+$ mass spectra of **1**–**9** display fragmentation peaks from [M – X]$^+$ and [M – X – L]$^+$. For all spectra, the isotopic patterns agree well with the calculated ones (see next section for HRESI-MS and molar conductivities for **1**–**9** measured in time). In the IR spectra of solid samples, any of one **1**–**9** exhibit a broad absorption band at 2250–2260 cm^{-1} that is shifted *vs.* the corresponding free cyanamides (2212–2222 cm^{-1}). This shift could be rationalized by existing of the cyanamide ligands mainly in the mesomeric structure N≡C–NR$_2$ with a low contribution of the cumulene-like form N$^-$=C=N$^+$R$_2$.[12] These conclusions, that are based upon the IR data, are well supported by X-ray diffraction study (see later). The high frequency shift of ν(C≡N) band of the coordinated cyanamides relatively to the corresponding uncomplexed species (*ca*. 40 cm^{-1}) – comparable with those for some other transition metal complexes with metal centers in average oxidation states – indicates a moderate electrophilic activation of NCNR$_2$ via coordination.[12] In the ^{1}H NMR spectra of **1**–**9**, all signals are low frequency shifted (by *ca*. 0.2 ppm) compared to the corresponding free NCNR$_2$ and these observations are in agreement with the literature data.[12]

In the molecular structures of **1**–**3**, **8**, and **9** (**Figure 1** and **Figures S1**–**S4** of ESI), the coordination polyhedra of the Zn atoms exhibit tetrahedral geometries (**Table 1**). The Zn–X and Zn–N distances are specific for the Zn–Cl (*ca*. 2.15–2.20), Zn–Br (*ca*. 2.35–2.36), Zn–I (*ca*.

2.54–2.56), and Zn–N (*ca.* 2.00–2.05 Å) bonds in the closely related $[ZnX_2(NCR)_2]$ species featuring conventional nitrile ligands.[31,34,35] The Zn–N bond length for **8** and **9** (2.037(2) and 2.041(2) Å, respectively) bearing the coordinated $NCNPh_2$ are slightly longer than those for complexes **1**–**3** having the $NCNMe_2$ ligands (2.010(4)–2.0259(17) Å; **Table 1**).
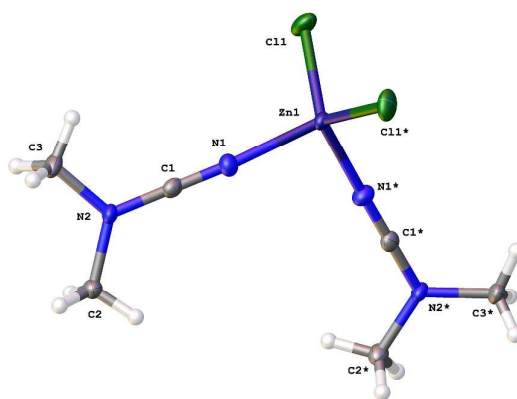

Figure 1. View of **1** with the atomic numbering scheme; one of two nonequivalent molecules is displayed. Thermal ellipsoids are given at the 50% probability level.

Table 1. Selected bond lengths [Å] and angles [°] for zinc complexes **1**–**3**, **8**, and **9**.

Parameter	1	2	3	8	9
Zn(1)–N(1)	2.0259(17)	2.010(4)	2.0119(16)	2.037(2)	2.041(2)
Zn(1)–N(1)*				2.044(2)	2.038(2)
Zn(1)–X(1)	2.2068(5)	2.3615(6)	2.5601(4)	2.3478(4)	2.5449(4)
Zn(2)–X(2)	2.1521(5)	2.3573(6)		2.3488(4)	2.5331(4)
N(1)–C(1)	1.151(3)	1.141(5)	1.145(3)	1.155(3)	1.145(4)
N(1)*–C(1)*				1.149(3)	1.144(4)
C(1)–N(2)	1.300(3)	1.332(9)	1.303(3)	1.321(3)	1.310(4)
C(1)*–N(2)*				1.326(3)	1.319(4)
N(2)–C(3)	1.435(2)	1.458(9)	1.467(2)		
N(2)–C(2)	1.459(3)	1.515(9)	1.466(2)		
N(1)*–Zn(1)–N(1)	103.76(10)	104.6(2)	99.94(10)	97.99	97.99(10)
X(2)–Zn(1)–X(1)	116.32(3)	116.49(4)	117.594(13)	122.245(17)	123.573(14)
N(1)–Zn(1)–X(1)	112.66(5)	108.33(12)	110.37(5)	110.61(7)	111.48(7)
N(1)*–Zn(1)–X(1)	105.43(5)	109.23(12)	110.38(5)	107.81(6)	110.92(7)
N(1)*–Zn(1)–X(2)	112.66(5)	108.33(12)	108.54(5)	111.84(6)	103.24(7)
C(1)–N(1)–Zn(1)	173.2(2)	173.4(4)	176.1(2)	159.4(2)	171.8(2)
C(1)*–N(1)*–Zn(1)				169.5(2)	159.1(2)
N(1)–C(1)–N(2)	178.8(2)	177.3(5)	178.4(2)	179.3(2)	179.2(3)
N(1)*–C(1)*–N(2)*				179.3(2)	179.2(3)

All NCNR$_2$ ligands exhibit end-on coordination mode. In **1**–**3**, the C–N–Zn fragments are almost linear with the angles of 173.2(2) (**1**), 173.4(4) (**2**), 176.1(2)° (**3**), while in **8** and **9** these angles demonstrate larger deviation from the linearity (159.4(2) and 169.5(2)° for **8** and 159.1(2) and 171.8(2)° for **9**; in each case values are given for two independent molecules). Quantum-chemical calculations (see below) indicate that, in the gas phase, isolated molecules of [ZnX$_2$(NCNR$_2$)$_2$] (**1**, **2**, **7**, **8**) should adopt the bent C–N–Zn arrangement. The observed linear configuration of the C–N–Zn fragments found by X-ray for **1**–**3** and non-equivalency of the NCNPh$_2$ ligands in **8** and **9** are probably due to packing effects. All bond lengths and angles of cyanamide ligands are the same, within 3σ, as those previously described.[12] Noticeably, that the most significant deviation from the linearity in similar systems was reported for [SbCl$_5$(NCNiPr$_2$)] (Sb–N–C is 133(1)°).[12,21]

Theoretical consideration. In order to better understand reasons of the different geometry of the C–N–Zn fragment in **1**–**3** and **8**, **9**, quantum-chemical calculations of **1**, **2**, **7**, and **8** have been carried out at the DFT level of theory (M06-2X and B3LYP). Experimental molecular geometry of the cyanamide complexes, in general, and that of the C–N–Zn fragment, in particular, is determined by the electronic structure, intramolecular, and intermolecular

7

(crystal packing) interactions. To separate the effects of the electronic structure and intramolecular interactions from the crystal packing effects, the calculations were performed for the isolated molecules. The experimental X-ray geometry of **2** was used as a starting point for the theoretical optimization procedure of **1** and **2**. As a result, the equilibrium structures of the C_{2v} symmetry with the C–N–Zn angles of 141.1–141.5° were obtained at the B3LYP level (**Figure 2**). The calculations using the M06-2X functional, which describes weak dispersion forces more adequately than B3LYP, resulted in the less symmetric equilibrium structures of **1** and **2** (C_2 symmetry) with the C–N–Zn angles of 110.3–112.5°. The lower angle in this case can be explained by the intramolecular interactions between the hydrogen atoms of the methyl groups and the halogen atoms (**Figure 2**) with the Cl/Br•••H distances of 2.922–2.972/3.086–3.127 Å, which were found at M06-2X but were not revealed at B3LYP. The results of the topological analysis of the electron density distribution (AIM) shows the presence of the bond critical points (BCPs) for these Cl/Br•••H contacts with the ρ, $\nabla^2\rho$, and H_b values of 0.044–0.050 e/Å^3, 0.446–0.557 e/Å^5, and (+0.005)–(+0.007) Hartree/Å^3. The low electron density and positive $\nabla^2\rho$ and H_b values at these BCPs indicate that the Cl/Br•••H interactions are weak and of the closed-shell type,[36] although they can contribute to the bending of the C–N–Zn fragment in the isolated molecules of **1** and **2**.

1, B3LYP

1, M06-2X

7, asymmetric
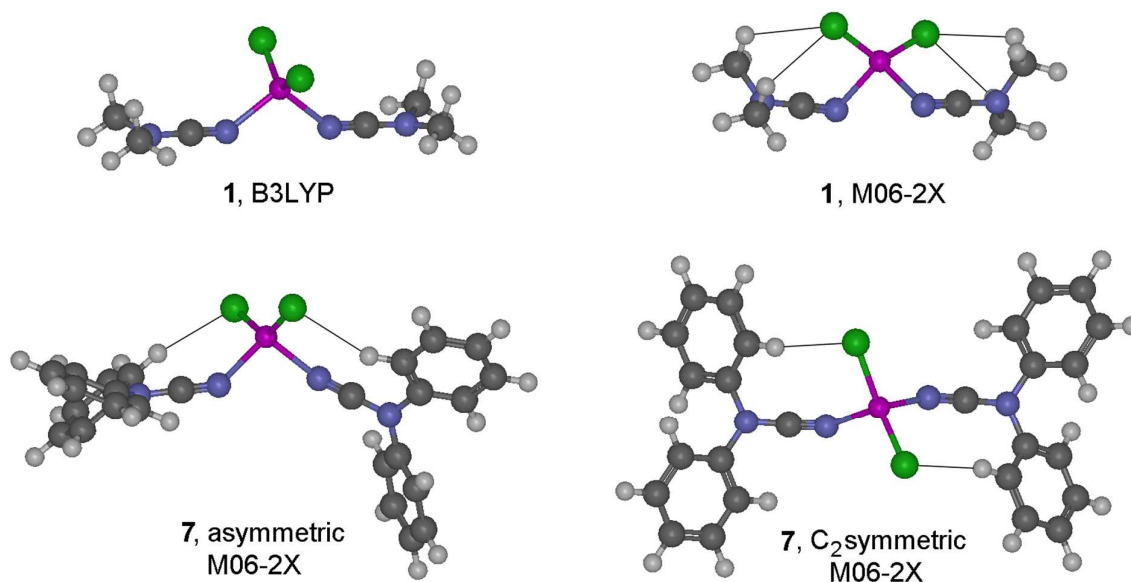M06-2X

7, C_2 symmetric
M06-2X

Figure 2. Equilibrium structures of **1** and **7**.

The optimization of **7** and **8** at both B3LYP and M06-2X levels starting from the X-ray geometry of **8** also led to the equilibrium structures with the bent C–N–Zn fragments (**Figure 2**). The non-equivalency of two NCNPh$_2$ ligands found by X-ray crystallography in the solid state is also preserved in the equilibrium structures of the isolated molecules. One of the calculated C–N–Zn angles is 148.1° (**7**, B3LYP), 153.6° (**7**, M06-2X), 159.1° (**8**, B3LYP), or 157.9° (**8**, M06-2X), while another angle is 140.4° (**7**, B3LYP), 140.1° (**7**, M06-2X), 142.8° (**8**, B3LYP), or 133.6° (**8**, M06-2X).

Both structures **7** and **8** were also optimized at M06-2X starting from the C$_2$ symmetric geometries. This symmetry was preserved during the optimization (**Figure 2**), both cyanamide ligands being equivalent with the C–N–Zn angles of 142.2° (**7**) and 143.8° (**8**). The C$_2$ symmetric structures are only slightly more stable than the corresponding asymmetric ones by (0.4–0.7 kcal/mol). All calculated structures **7** and **8** are stabilized by the intramolecular interactions between the Ph groups and the halogen atoms with the Cl/Br•••H distances of 2.729–2.767/2.911–2.977 Å (M06-2X). These interactions may contribute to the bending of the C–N–Zn fragment in the isolated complexes **7** and **8**.

Location of two, C$_2$ symmetric and asymmetric, structures for **7** and **8** may be accounted for by the steric interaction between the geminal phenyl groups. Such an interaction hampers free rotation around the N–C$_{Ph}$ bonds and, thus, provides the existence of two minima on the potential energy surface. In the case of **1** and **2**, the interaction between the geminal methyl groups is not significant and the free rotation around the N–C$_{Me}$ bonds leads to the degeneration of two minima into one corresponding to the most stable conformation.

The computational results indicate that in the isolated molecules the C–N–Zn fragments are always significantly bent independently on the substituent R of the cyanamide ligand

NCNR$_2$. Thus, the nearly linear geometry of the C–N–Zn fragments found by X-ray in the solid state of **1**–**3** may be accounted for by the packing effects, which result in their straightening.

The electronic structure of complexes **1**–**9** should be considered as intermediate between two resonance forms of the cyanamide ligands, *i.e.* the nitrile form N≡C–NR$_2$ (**a**) and the cumulene-like form N$^-$=C=N$^+$R$_2$ (**b**). The natural bond orbital (NBO) analysis (M06-2X) revealed that the nitrile resonance form **a** is the predominant one, while the cumulene-line form **b** provides lower but noticeable contribution (*e.g.*, the non-Lewis occupancies of these resonance forms in **1** are 0.93% and 1.40%, respectively). Correspondingly, the calculated bond order (Wiberg bond index) of the N(1)C(1) bond in **1**, **2**, **7**, and **8** is 2.62–2.69.

For the resonance form **a**, three CN bond orbitals associated with the nitrile group, one NBO of the C(1)–N(2) single bond and the lone electron pair at the N(2) atom were found for each ligand in all calculated structures (**Table 2**). For the resonance form **b**, two NBOs for each N(1)C(1) and C(1)N(2) bonds were located. The Zn–Hal and Zn–N bond orbitals were also found in complexes **1** and **2**, whereas no such orbitals were detected in **7** and **8** indicating conceivable predominant Coulomb-type metal-ligand interactions.

Table 2. Results of the NBO analysis of **2** at the M06-2X level.[a]

Bond orbital		Nitrile form **a**	Cumulene-like form **b**
Zn–Br	occ.	1.98	1.98
	%Zn	15.07, sp$^{2.06}$	15.07, sp$^{2.06}$
	%Br	84.93, sp$^{2.75}$	84.93, sp$^{2.75}$
Zn–N(1)	occ.	1.92	1.96
	%Zn	6.95, sp$^{4.65}$	6.03, sp$^{4.65}$
	%N	93.05, sp$^{0.81}$	93.97, sp$^{0.54}$
N(1)C(1) (σ)	occ.	1.99	1.99
	%N	57.33, sp$^{2.03}$	57.28, sp$^{2.01}$
	%C	42.67, sp$^{0.90}$	42.72, sp$^{0.90}$
N(1)C(1) (π)	occ.	1.98	1.98
	%N	67.30, sp$^{7.37}$	55.78, p
	%C	32.70, p	44.22, p
N(1)C(1) (π)	occ.	1.98	–
	%N	55.79, p	–
	%C	44.21, p	–
C(1)N(2) (σ)	occ.	1.98	1.98
	%N	60.59, sp$^{1.97}$	60.53, sp$^{1.98}$

	%C	39.41, sp$^{1.12}$	39.47, sp$^{1.13}$
C(1)N(2) (π)	occ.	–	1.95
	%N	–	82.82, p
	%C	–	17.18, p

[a] Ratios of the p and s contributions in the hybrid orbitals are shown in superscript.

Analysis of the atomic orbitals contribution in NBOs of **2** demonstrates that p-orbital of the metal mostly participates in the Zn–N NBO (sp$^{4.65}$ hybridization), while an orbital of the N atom with predominant s character contributes to this bond (**Table 2**). The hybridization of the carbon orbital in the N(1)C(1) σ NBO is close to the sp type. However, the nitrogen orbital is sp^2 hybridized in both forms **a** and **b**. All these results indicate that the bent structure of the C–N–Zn fragment is associated with the rehybridization of the N orbital forming the N(1)C(1) bond and with the increased contribution of the cumulene-like resonance form **b** which, nevertheless, is not the predominant one.

Ligand redistribution in 1–9. Molar conductivity measured for **1–9** in CH$_2$Cl$_2$ at RT demonstrates that these complexes behave as nonelectrolytes and the conductivity of these solutions, kept in closed flasks, is stable for at least 1d. The HRESI$^+$-MS of these solutions measured after 1d correspond to the starting HRESI$^+$-MS of **1–9**, *i.e.* display sets of signals from [M – X]$^+$ and [M – X – L]$^+$.

Upon dissolution of **7–9** in non-dried CH$_2$Cl$_2$, we succeeded the identification of the [Zn(NCNPh$_2$)$_4$]$^{2+}$ ions in the HRESI-MS spectra (observed *m/z* 420.1327; required 420.1334). Substantial dilution of the solution along with prolonged keeping in air leads to increasing intensities of these peaks. Moreover, in the presence of excess NCNPh$_2$ intensity of [Zn(NCNPh$_2$)$_4$]$^{2+}$ become substantially higher. In the HRESI-MS$^-$ of **7–9** in CH$_2$Cl$_2$, intensive signals of [ZnX$_3$]$^-$ were detected and these intensities are even more increased when reaction mixtures were kept in air for a week.

In accord with these experiments, when dichloromethane solutions of **7** or **8** were subject to slow (for approximately two weeks) evaporation in moistures air, we isolated the new zinc

complexes $[Zn(NCNPh_2)_4(H_2O)_2][Zn_2(\mu-X)_2X_4]$ (X = Cl **10**, Br **11**) as the solids in small non-preparative quantities and, after mechanical separation, characterized these species by X-ray crystallography (**Figure 3** and **Figure S5**, see ESI), HRESI-MS, and ^1H NMR. We believe that concentration of **10** or **11** in the solutions is small, but their solubility is poor as they are formed by a successful combination of "large cation—large anion"[37] and, in addition, the 2$^+$-charges on the counterions also minimize the solubility.[38] We were able to improve the yield of **11** (54%) when the reaction between $ZnBr_2$ and $NCNPh_2$ was performed in a 3:4 molar ratio, while for system $ZnCl_2/NCNPh_2$ mixture of products was obtained under the same conditions.

In the HRESI-MS$^+$ of **10** and **11**, the most intensive peak corresponds to $[Zn(NCNPh_2)_4]^{2+}$ (*m/z* 420.1327; requires 420.1334), whereas in the HRESI-MS$^-$ of **10** and **11** peaks 170.8339 ($[ZnCl_3]^-$ requires 170.8328) and 306.6974 ($[Zn_2Cl_5]^-$ requires 306.6965), 304.6724 ($[ZnBr_3]^-$ requires 304.6790), and 528.4331 ($[Zn_2Br_5]^-$ requires 528.4428), respectively, were detected.

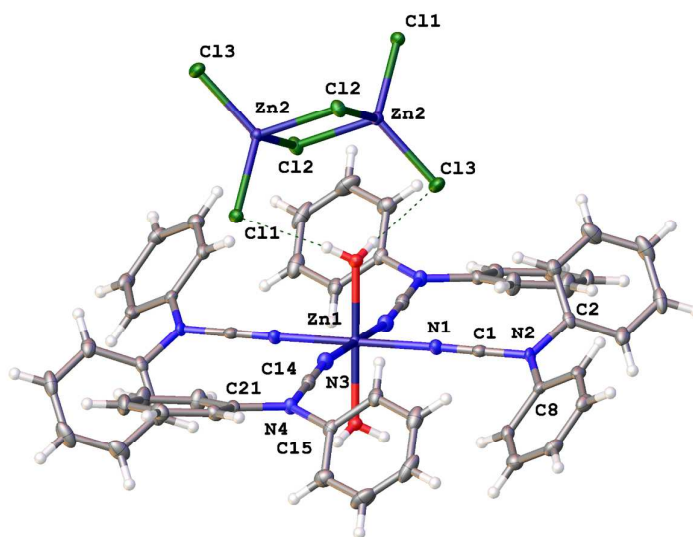**Figure 3**. View of $[Zn(NCNPh_2)_4(H_2O)_2][Zn_2(\mu-Cl)_2Cl_4]$ (**10**). Selected bond distances (Å) and angles (°): Zn(1)–N(1) 2.126(2), Zn(1)–N(3) 2.108(2), N(1)–C(1) 1.146(3), N(3)–C(14) 1.149(3), N(4)–C(14) 1.318(3), N(2)–C(1) 1.327(3), Zn(1)–N(1)–C(1) 178.3(2), C(1)–N(2)–C(2)
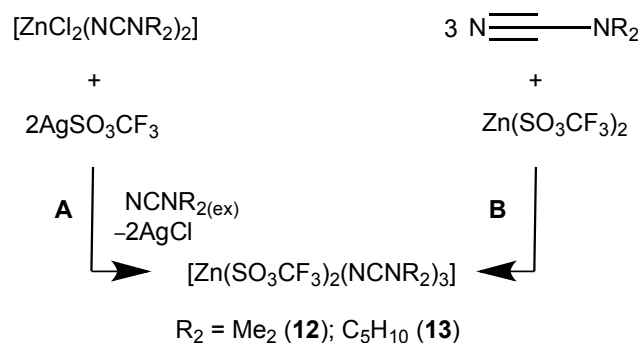
117.8(2), C(1)–N(2)–C(8) 117.4(2), C(2)–N(2)–C(8) 123.5(2), Zn(1)–N(3)–C(14) 165.7(2),

N(1)–Zn(1)–N(3) 88.63(7), N(3)–Zn(1)–N(3) 180.00(7), Zn(1)–N(3)–C(14) 165.7(2)

Structures of **10** (**Figure 3**) and **11** (**Figure S5**, ESI) are composed of the 2^+-charged

counterions. The Zn atom in the $[Zn(NCNPh_2)_4(H_2O)_2]^{2+}$ complex has an octahedral

environment with two *trans*-located molecules of water. The Zn–O bond lengths exhibit values

typical for the known octahedral zinc aqua complexes.[39–43] Diphenylcyanamide ligands lie in the

equatorial plane forming the equivalent pairs. Molecules of one pair exhibit slightly bent

fragment with the C(1)–N(1)–Zn angle 178.3(2)° for **10** and of 175.5(6)° for **11**, and the

relatively large torsion angle C(2)–N(2)–Zn(1)–N(3) of –35.5° for **10** and –145.6° for **11**.

Another pair is characterized by the C(14)–N(3)–Zn angle of 165.7(2)° for **10** and 165.2(6)° for

11 and the torsion angle C(15)–N(4)–Zn(1)–N(1) of 10.9° for **10** and –14.8 for **11**. The Zn(1)–

N(1) bonds of the first pair are longer than the Zn(1)–N(3) bonds (*ca.* 0.018–0.042 Å for **10** and

0.045 Å for **11**), other bonds differences are smaller (Δl less than 0.017 Å). All bond lengths and

angles of diphenylcyanamide ligands are the same, within 3σ, as those for **8** and **9**. The bond

length and angles of the $[Zn_2(\mu\text{-}X)_2X_4]^{2-}$ anionic parts of **10** and **11** are typical for this type

dinuclear anionic species,[44] whereas the angle Zn–Cl–Zn is slightly shorter (93.2 in **11** vs. *lit.*[44]

95.0°).

Generation of halide-free zinc cyanamide species $[Zn(CF_3SO_3)_2(NCNR_2)_3]$. We

attempted the synthesis of (cyanamide)Zn^{II} complexes bearing more than two coordinated

$NCNR_2$ ligands and having coordination number greater than four. Thus, we performed reaction

of $NCNR_2$ with the halide-free zinc precursor $Zn(CF_3SO_3)_2$. We assumed that a weakly bound

$CF_3SO_3^-$ could be easily substituted by cyanamides and this could lead to increasing number of

coordinated $NCNR_2$ species.

The systems $Zn(CF_3SO_3)_2/NCNR_2$ (R_2 = Me_2, C_5H_{10}) were monitored by HRESI$^+$-MS at

different molar ratios of the reagents (1:3 and 1:4). For all combinations of the reactants

intensive signals from the $[Zn + 3NCNR_3 + CF_3SO_3]^+$ ions were observed in HRESI$^+$-MS, whereas species exhibiting $Zn/NCNR_2$ ratio greater than 1:3 were not observed.

$$[ZnCl_2(NCNR_2)_2] \qquad\qquad 3\ N{\equiv\!\!\equiv}NR_2$$

$$+ \qquad\qquad\qquad\qquad +$$

$$2AgSO_3CF_3 \qquad\qquad\qquad Zn(SO_3CF_3)_2$$

A | NCNR$_{2(ex)}$ / –2AgCl   B

$$[Zn(SO_3CF_3)_2(NCNR_2)_3]$$

$$R_2 = Me_2\ (\mathbf{12});\ C_5H_{10}\ (\mathbf{13})$$

Scheme 2. Synthesis of $[Zn(CF_3SO_3)_2(NCNR_2)_3]$ (**12**, **13**).

Halide-free zinc complexes featuring three cyanamide ligands, **12** and **13**, were prepared by two routes, *i.e.* by halide abstraction from complexes **1**, **2** (**Scheme 2**, method A) by 2 equivs AgCF$_3$SO$_3$ in the presence of 2-fold excess of NCNR$_2$ or by the reaction of NCNR$_2$ with Zn(CF$_3$SO$_3$)$_2$ (**Scheme 2**, method B). In the former case, the reactions were carried in a 1:2 molar ratio between either **1** or **2** and NCNR$_2$, respectively, in dry acetone solutions (RT, under Ar, vigorous stirring in the dark) for 2 h. After the completion, the acetone solutions were evaporated to dryness and the residues formed were treated with petroleum ether (40–70 °C) giving colorless crystalline powders of $[Zn(CF_3SO_3)_2(NCNR_2)_3]$ (R$_2$ = Me$_2$ **12**, C$_5$H$_{10}$ **13**; 76–79%). Complexes **12** and **13** were also prepared from zinc triflate and NCNR$_2$ in a 1:3 molar ratio in dry acetone (**12**, **13**) (RT, under Ar) and isolated in 83–85% yields. The reaction with 4-fold excess of NCNR$_2$ also lead to **12** and **13**, but their isolation is more difficult due to formation of oily residues, which were not crystallized under hexane, petroleum ether, Et$_2$O, or toluene. All attempts to prepare the similar complex $[Zn(CF_3SO_3)_2(NCNPh_2)_3]$ starting from NCNPh$_2$ gave a mixture of Zn-containing products and unreacted NCNPh$_2$.

Elemental analysis for Zn perfectly corresponds to $[Zn(CF_3SO_3)_2(NCNR_2)_3]$ for **12** and **13**. In the HRESI-MS$^+$ of **12** and **13**, both the $[Zn(SO_3CF_3)(NCNR_2)_3]^+$ and

$[Zn(SO_3CF_3)(NCNR_2)_2]^+$ ions were detected with isotopic patterns that agree well with the calculated ones. In the IR spectra, **12** and **13** exhibit two bands at 2265–2242 (br) and 2222–2231 cm^{-1}, which correspond to ν(CN) of the coordinated and the uncomplexed NCNR$_2$; the ligand NCNR$_2$ can be decoordinated from the complexes upon KBr pellets preparation. In the ATR spectra, both **12** and **13** exhibit a single band at 2253 cm^{-1} due to the CN stretches. In the ^{1}H NMR spectra of **12** and **13**, the ligand protons are low freqency shifted (by *ca.* 0.1 ppm) relative to the corresponding protons of the uncomplexed NCNR$_2$.

All attempts to grow crystals of **12** led to crystalline species having other compositions and the resulting complexes were characterized by single-crystal X-ray diffraction. Thus, crystals of $[Zn(NCNMe_2)_3(H_2O)_2](SO_3CF_3)_2$ (**12a**) were obtained from the starting $[Zn(CF_3SO_3)_2(NCNR_2)_3]$ (**12**) before workup with petroleum ether (see Experimental), which was spontaneously crystallized in an open vial. The crystals of $[Zn(CF_3SO_3)_2(NCNMe_2)_2]_\infty$ (**12b**) were obtained from **12** upon dissolution in dry CH$_2$Cl$_2$, followed by evaporation to dryness giving an oily residue that was partially crystallized at RT overnight.

Structure of **12a** is composed of the two CF$_3$SO$_3^-$ anions per one $[Zn(NCNMe_2)_3(H_2O)_2]^{2+}$ cation. The cation has a trigonal bipyramidal geometry and comprise of the two water molecules in the axial positions and the three NCNMe$_2$ ligands lying in one plane (**Figure 4**). The Zn–O bonds are similar to those in **10** and **11** and the Zn–N bonds for **10**, **11** (2.097–2.126 Å) are longer than those for **12a** (2.002–2.104 Å).

In **12b**, the zinc center exhibits an octahedral environment and this complex has a polymeric structure with triflate anions forming the bridges (**Figure 5**). The Zn–O bonds have values similar with those for other known Zn/triflate complexes,[45,46] and the Zn–N distances are close, within 3σ, to those in the (cyanamide)Zn species (**1–3**, **8**, **9–11**). In both **12a** and **12b**, the bond lengths in the dimethylcyanamide ligands are the same, within 3σ, as those in the other (dimethylcyanamide)Zn^{II} complexes, viz. **1–3**, and the angles Zn–N–C for **12a** and **12b** are

smaller (142.9(3)–167.1(3) Å for **12a**, 159.0(3) and 159.1(3) Å for **12b**) than for **1**–**3** (173.2(2)–
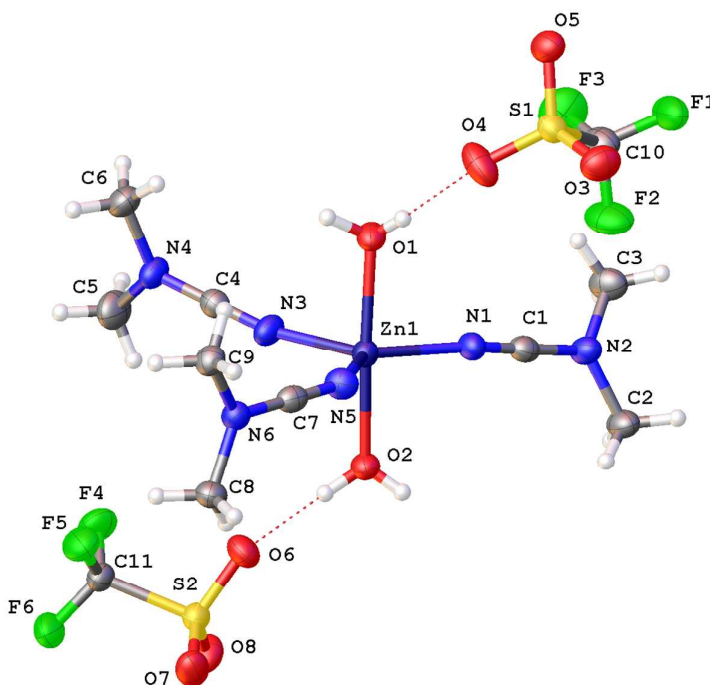
176.1(2)°).

Figure 4. View of [Zn(NCNMe$_2$)$_3$(H$_2$O)$_2$](SO$_3$CF$_3$)$_2$ (**12a**). Thermal ellipsoids are drawn at the

50% probability level. Selected bond distances (Å) and angles (°): Zn(1)–N(1) 2.006(3), N1–C1

1.141(4), C1–N2 1.304(4), C(7)–N(6) 1.298(4), Zn(1)–O(1) 2.104(3), Zn(1)–O(2) 2.084(3);

O(1)–Zn(1)–O(2) 173.8(1), N(5)–Zn(1)–N(1) 122.9(1), N(1)–Zn(1)–N(3) 127.0, N(3)–Zn(1)–

N(5) 110.1(1), C(1)–N(1)–Zn(1) 163.5(3), C(7)–N(5)–Zn(1) 142.9(3), C(4)–N(3)–Zn(1)

167.1(3), N(1)–C(1)–N(2) 177.5(3), N(5)–C(7)–N(6) 179.4(3), N(3)–C(4)–N(4) 179.6(3).
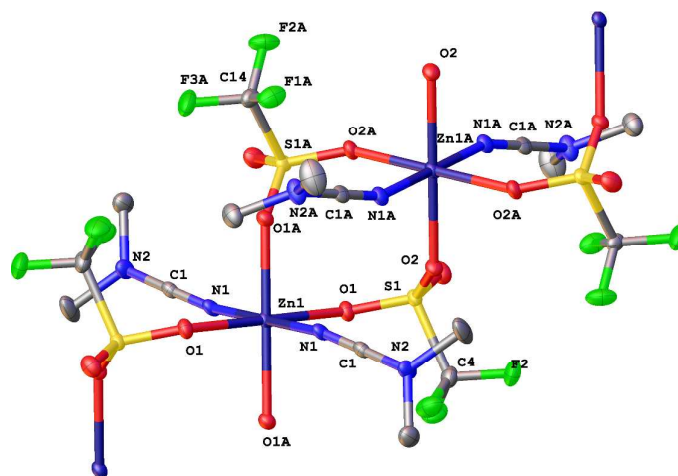
Figure 5. View of $[Zn(CF_3SO_3)_2(NCNMe_2)_2]_n$ (**12b**) with the atomic numbering scheme. Thermal ellipsoids are given at the 50% probability level (hydrogen atoms were omitted for clarity). Selected bond distances (Å) and angles (°): Zn(1A)–N(1A) 2.007(4), Zn(1)–N(1) 2.025(3), N(1A)–C(1A) 1.139(5), C(1A)–N(2A) 1.308(5), N(1)–C(1) 1.145(4), C(1)–N(2) 1.308(4), O(1)–Zn(1)–O(1A) 89.83(7), O(1)–Zn(1)–O(1) 180.00, O(1A)–Zn(1)–O(1A) 180.00, N(1)–Zn(1)–N(1) 180.0, Zn(1)–N(1)–C(1) 159.1(3), N(1)–C(1)–N(2) 177.8(3), Zn(1A)–N(1A)–C(1A) 159.0(3), N(1A)–C(1A)–N(2A) 179.7(3).

Thus, we demonstrated that the application of $Zn(CF_3SO_3)_2$ in the syntheses of cyanamide complexes led to zinc species bearing three ligands, viz. $[Zn(CF_3SO_3)_2(NCNR_2)_3]$ (R = Me$_2$, C$_5$H$_{10}$) (**12**, **13**). These complexes exhibit high lability and pronounced tendencies for ligand exchange. All these complicate the generation of the so-called well-defined complexes and we obtained, upon crystallization attempts, species of different composition. It should be mentioned that (nitrile)Zn^{II} complexes of the $[Zn(NCR)_3(H_2O)_2]^{2+}$ type were unknown before our experiments. In this context, it is worthwhile noticing that only one relevant structure, $[Zn(NCMe)_4]^{2+}$, where the zinc(II) center coordinates more than two nitrile species, was previously reported.[47] In the case of NCNPh$_2$, we were unable to isolate the pure complex and,

instead, we obtained mixtures of zinc complexes and the free cyanide. A possible reason is a lower donor ability of $NCNPh_2$ as compared to $NCNAlk_2$.

Zn^{II}-mediated hydration of cyanamide ligands. In the past decade, various hydration/hydrolysis reactions of NCR involving metal centers were subject of rapt attention (see reviews[4,48] and recent works[49–53]). One should mention that all so far known Zn-based systems for hydration of conventional NCR species require the presence of co-catalyst. In addition, no single example of Zn^{II}-mediated or Zn^{II}-catalyzed nitrile hydration of cyanamides was reported.

Thus, Kopylovich et al.[49] studied zinc(II)-catalyzed NCR hydration that was facilitated by addition of a ketoxime as co-catalyst and this methodology has synthetic utility for generation of a broad range of amides. The hydration requires the presence of both ZnX_2 and a ketoxime and the hydration does not proceed at all with either the zinc salt or with the ketoxime taken alone. It was proposed that $HON=CR'_2$ acts as a nucleophile and adds to zinc(II)-activated nitrile to form the $\{Zn–NH=C(R)ON=CR'_2\}$ intermediate, which was not detected. The formed imidoyloxime ligand hydrolyzes giving appropriate carboxamide and this hydration is accompanied with elimination of the oxime. Later, Lu et al.[54] used the $[Zn^{II}]/MeC(H)=NOH$ systems for catalytic hydration of nitriles bearing aromatic and heteroaromatic substituents and Pasha et al.[55] reported that NCAr can be converted under MW irradiation into the corresponding amide NH_2COAr in good yield by using catalytic $ZnCl_2$/acetamide system in H_2O/THF media.

In current study, we also observed the hydration of cyanamides, but this reaction is metal-mediated rather than metal-catalyzed. In these experiments, we isolated corresponding ureas and their derivatives and found that the hydration does not require any co-catalyst (oximes or amides) to enhance the addition of H_2O. Thus, the zinc(II)-mediated hydration of the cyanamides was carried out with the systems comprised of ZnX_2 (X = Cl, Br, I) and 2 equiv any of one $NCNR_2$ (R_2 = Me_2, C_5H_{10}, Ph_2) in all possible combinations and *ca.* 40-fold excess of water in acetone at 60 °C (R_2 = Me_2, C_5H_{10}) or 80 °C (R_2 = Ph_2) in closed vials. The conversion of nitriles to the appropriate ureas was monitored by IR spectroscopy that indicated the disappearance of

the CN stretches (2250–2220 cm^{-1}) of the cyanamide species and, eventually, completeness of the hydration was achieved after *ca.* 3 d (R$_2$ = Me$_2$, C$_5$H$_{10}$) and in case of (R$_2$ = Ph$_2$) the hydration completeness achieved only under heating at higher temperature (80 °C) for 1 d. The complexes [ZnX$_2${OC(NR$_2$)NH$_2$}$_2$] (X = Cl, Br, I; R$_2$ = Me$_2$, C$_5$H$_{10}$; **14**–**19**) were obtained as colorless crystalline solids in moderate to good yields (60–81%; **Scheme 3**). The [ZnX$_2${OC(NPh$_2$)NH$_2$}] (X = Cl, Br) (**20**, **21**) species were purified by column chromatography and obtained in 57 and 69% yields, correspondingly, while [ZnI$_2${OC(NPh$_2$)NH$_2$}$_2$] (**22**) decomposes on SiO$_2$ and it was characterized by HRESI$^+$-MS and ^{1}H NMR in the reaction mixture. Complexes **20** and **21** contain an admixture of OC(NPh$_2$)NH$_2$ (*ca.* 40:1 mol/mol), which was not separated, and **20** and **21** were characterized by HRESI-MS, IR, ^{1}H and ^{13}C{^{1}H} NMR. We also observed that Zn(SO$_3$CF$_3$)$_2$ promotes hydration of cyanamides, but the hydration proceeds slower and less selective (in NCNR$_2$/H$_2$O at 60 °C hydration products were detected after 4 d along with unreacted NCNR$_2$) than for ZnX$_2$-based (X = Cl, Br, I) systems and Zn(SO$_3$CF$_3$)$_2$ could not be recommended for efficient hydration of NCNR$_2$.
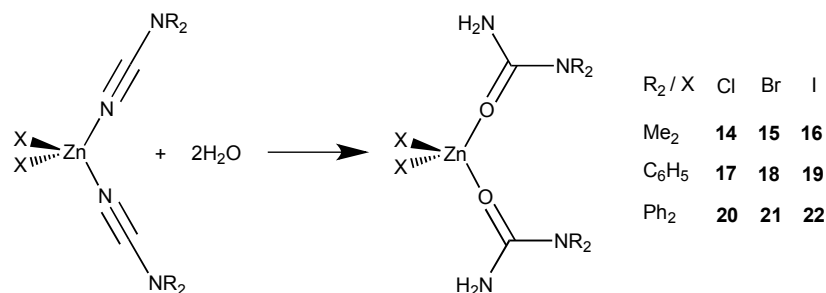
Scheme 3. Hydration of the Zn-coordinated cyanamides.

Complexes **14**–**19** give satisfactory Zn analyses for the proposed formulae and were also characterized by HRESI-MS, IR, and ^{1}H, ^{13}C{^{1}H} NMR spectroscopies. The IR spectra of **14**–**21** are in agreement with those previously reported for the *N,N*-dimethyl- and *N,N*-diethylurea zinc(II) complexes[56,57] and exhibit medium-to-strong bands at 3433–3482 cm^{-1} that can be

attributed to the N–H stretches. The spectra also display one or two overlapped ν(C=O) stretches in the ranges of 1626–1637 cm^{-1} and 1648–1658 cm^{-1}; the former band is low-field shifted as compared to those observed for uncomplexed urea derivatives (*ca*. 1650–1660 cm^{-1}); this low-field shift is typical for *O*-bound ureas.[56] No bands assignable to the C≡N stretches from the (cyanamide)Zn^{II} species were observed.

The HRESI$^+$ mass-spectra display peaks corresponding to the fragmentation ions [M – X]$^+$ with the characteristic isotopic pattern. In the ^{1}H NMR spectra of **14–22**, one set of signals, which corresponds to the coordinated ureas, was observed. The characteristic feature of the ^{1}H NMR spectra of **14–22** is the presence of one broad signal in a low frequency region recognized as the NH$_2$ resonance. The ^{13}C{^{1}H} NMR spectra of **14–21** display signals of *C*=O at low frequency (*ca*. 160 ppm).

The structures of four complexes, **14–16** and **18**, were confirmed by X-ray crystallography. The structures of **14–16**, prepared by the direct treatment of ZnX$_2$ with the *N,N*-dimethylurea are known[57,58] therefore in Experimental part we give only structural parameters for these complexes and supply the complete cif-files in ESI and here we provide only description of the unknown structure of **18** (**Figure 7**).

In the molecular structure of **18**, the coordination polyhedron of the zinc atom exhibits a tetrahedral geometry. The Zn–Br and Zn–O distances are specific for the Zn–Br and Zn–O bonds in the [ZnX$_2${OC(NMe$_2$)NH$_2$}$_2$] species[57,59] (see also ESI for parameters of **14–16**, **Figures S7–S9** and **Table S5**). The C–O bond lengths are the typical C=O double bonds and their values are similar, within 3σ, with those in other (urea)Zn^{II} complexes (see ESI and ref.[57]) and in uncomplexed *N,N*-dimethylurea.[60] The C(5)–N and C(8)–N bond distances [from 1.330(4) to 1.338(4) Å] have intermediate order due to the conjugation and their bond lengths are coherent with those in other (urea)Zn^{II} species (see ESI and refs.[57]) and in uncomplexed *N,N*-dimethylurea.[60] The intramolecular hydrogen bond is formed between the amide group of one urea ligand and the oxygen atom of the other urea ligand (N–H•••O 2.921 Å).
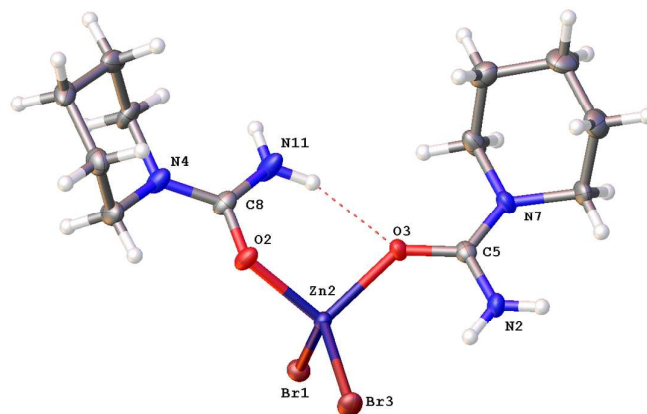
Figure 7. View of $[ZnBr_2\{OC(NC_5H_{10})NH_2\}]$ (**18**) with the atomic numbering scheme. Thermal ellipsoids are given at the 50% probability level. Selected bond lengths (Å) and angles (°): Zn(2)–Br(1) 2.3837(5), Zn(2)–Br(3) 2.3349(5), Zn(2)–O(2) 1.951(2), Zn(2)–O(3) 1.994(2), O(3)–C(5) 1.272(3), C(5)–N(7) 1.331(4), C(5)–N(2) 1.345(4), O(2)–C(8) 1.270(4), C(8)–N(11) 1.338(4), C(8)–N(4) 1.330(4); Br(1)–Zn(2)–Br(3) 114.78(2), Br(3)–Zn(2)–O(3) 115.97(6), Br(3)–Zn(2)–O(2) 110.24(6), Zn(2)–O(2)–C(8) 126.3(2), Zn(2)–O(3)–C(5) 132.1(2), O(2)–C(8)–N(11) 119.3(3), O(2)–C(8)–N(4) 120.2(3), O(3)–C(5)–N(2) 119.7(3), O(3)–C(5)–N(7) 120.4(3).

Hydration of conventional nitriles and cyanamides at soft metal centers, *e.g.* platinum, leads to *N*-coordinated amides and ureas in their iminol form.[61,62] In this work, we observed formation of zinc complexes featuring the expected[63] *O*-coordinated ureas. Hydration seems to occur at the zinc-activated cyanamide C atom giving the iminol complex $[ZnX_2\{HN=C(OH)NR_2\}_2]$, which then undergoes the linkage isomerization accompanied with the tautomerization of the ligands to furnish the *O*-bound urea derivative $[ZnX_2\{OC(NH_2)NR_2\}_2]$.[64] From a viewpoint of HSAB theory, zinc(II) metal center is hard acid and tends to ligate the O rather than the N urea centers. Quantum-chemical calculations

performed for the urea-containing *N,N'*-bis(*m*-ethoxycarbonylphenyl)Zn[II] complexes are in complete agreement with this statement.[65]

Hydration of cyanamides is metal-mediated insofar as in the blank experiment we established that in the absence of zinc salts the cyanamides $NCNR_2$ ($R_2 = Me_2$, C_5H_{10}, Ph_2) do not convert to the corresponding ureas upon heating for 3 d at 60 °C in acetone with H_2O. In contrast to the previously known Zn[II]-mediated hydration of conventional nitriles, the reaction with cyanamides does not require any co-catalyst. Interestingly that hydration of nitriles NCR (R = Et, Ph) does not proceed under conditions of Zn[II]-mediated cyanamide hydration ($ZnCl_2/H_2O_{excess}$ in acetone at 60 °C for 3 d) and this observation is in accord with our previous findings showing that $NCNR_2$ species are more reactive toward nucleophilic attack than NCR's.[12,66]

In our work, we observed zinc(II)-mediated hydration of cyanamides, which does not require any co-catalyst. Known examples of metal-mediated hydration of dialkylcyanamides include catalytic generation of *N,N*-dialkylureas in presence of H_2WO_4 that acts as solid acid catalyst[67] and catalytic hydration of cyanamides with mercury salts in acidic media.[68] Other examples of metal-mediated hydration of cyanamides were found at Pt[II], Pt[IV], Os[III], and Co[II] centers.[69,70]

Final Remarks

The result of this work can be considered from a few perspectives. First, we developed a general synthetic procedure and synthesized a family of the non-electrolyte zinc(II) complexes $[ZnX_2(NCNR_2)_2]$ featuring two cyanamide ligands. Despite Zn[II] is, in general, a labile metal center, these compounds are well-defined and stable species under anhydrous conditions and can be conveniently applied for generations of other zinc complexes. We also observed that $[ZnX_2(NCNPh_2)_2]$ (X = Cl, Br) are rather moisture-sensitive and slowly undergoes ligand

redistribution in solutions forming the ionic species $[Zn(NCNPh_2)_4(H_2O)_2][Zn_2(\mu-X)_2X_4]$. Moreover, prolonged heating of $[ZnX_2(NCNR_2)_2]$ in wet solvents results in metal-mediated hydration of $NCNR_2$ followed by the isomerization/tautomerization of the formed hypothetical iminols, $HN=C(OH)NR_2$, giving *O*-bound ureas, $O=C(NH_2)(NR_2)$. All these ligand redistribution and hydration processes should be taken into account when $[ZnX_2(NCNR_2)_2]$ are employed as starting materials for synthetic experiments.

Second, we synthesized and characterized the halide-free zinc(II) complexes $[Zn(CF_3SO_3)_2(NCNR_2)_3]$ ($R_2 = Me_2$, C_5H_{10}) and found that these species exhibit substantial lability. The latter phenomenon become obvious when, in particular, we attempted to grow X-ray quality crystals of $[Zn(CF_3SO_3)_2(NCNMe_2)_3]$ and all our crystallizations, albeit performed at RT, led to compounds of different compositions such as the ionic $[Zn(NCNMe_2)_3(H_2O)_2](SO_3CF_3)_2$ and the polymeric $[Zn(CF_3SO_3)_2(NCNMe_2)_2]_\infty$ complexes. Although the lability of metal complexes in many instances complicates the synthetic[55] procedures, the labile halide-free $[Zn(CF_3SO_3)_2(NCNR_2)_3]$ compounds could be used for facile substitution reactions and preparation of metal-polymeric species.

Third, despite the hydration of zinc(II)-activated conventional nitriles was studied earlier, [49,54,71] the hydration of Zn^{II}-bound cyanamides was observed for the first time. We demonstrated that the reaction – in contrast to the reported Zn^{II}-involved hydrations of conventional NCR species – does not require addition of any co-catalyst to facilitate the addition of H_2O. Therefore, cyanamides $NCNR_2$ appear to more activated by zinc(II) centers and their reactivity toward hydration is greater than those of conventional nitriles NCR; this statement is well coherent with our previous findings.[12,14,15]

Forth, we synthesized transition metal complexes of $NCNPh_2$, viz. $[ZnX_2(NCNPh_2)_2]$ (X = Cl, Br, I) and observed reactivity of zinc(II)-coordinated $NCNPh_2$ toward nucleophilic addition exemplified by the hydration. In all X-ray structures of the $(NCNPh_2)Zn^{II}$ species (**7**, **8**, **10**, and

11), the Zn–N–C fragment demonstrated some deviation from linearity (angles Zn–N–C are *ca.* 146–178° in **7**, **8**, **10**, and **11**).

Fifth, theoretical calculations at the DFT level of theory demonstrated that the Zn–N–C fragment is clearly bent in the isolated molecules of both dialkyl- and diarylcyanamide complexes. The linear geometry of this fragment in the solid state of **1**–**3** may be accounted for by packing effects. The angular distortion in the isolated molecules is associated with the rehybridization of the nitrogen hybrid orbital forming the CN nitrile σ bond (sp^2 type instead of the sp type) and with the increased contribution of the cumulene-like resonance form $N^-=C=N^+R_2$ which, nevertheless, is not the predominant one. Intramolecular interactions between groups R and the halogen atoms also contribute to the bending of the Zn–N–C fragment.

Experimental

Materials and Instrumentation. Solvents, $ZnCl_2$, $ZnBr_2$, and $Zn(CF_3SO_3)_2$ were obtained from commercial sources and used as received apart from dichloromethane and acetone that for some experiments were dried by distillation over P_4O_{10}. ZnI_2 was prepared from Zn dust and iodine in dry diethyl ether as described.[72] Diphenylcyanamide was obtained by the known procedure,[73,74] while the other cyanamides were purchased from Sigma-Aldrich. A standard EDTA method was employed for Zn analysis.[75] The HRESI mass-spectra were obtained on a Bruker micrOTOF spectrometer equipped with electrospray ionization (ESI) source; CH_2Cl_2 or MeOH were used as the solvents. The instrument was operated in positive or negative ion mode using an *m/z* range of 50–3000. The capillary voltage of the ion source was set at –4500 V (ESI^+) and the capillary exit at $\pm$(70–150) V. The nebulizer gas pressure was 0.4 bar, and the drying gas flow was 4.0 L/min. The most intense peak in the isotopic pattern is reported. Infrared spectra (4000–400 cm^{-1}) were recorded on a Shimadzu FTIR 8400S instrument in KBr pellets. ATR FT-IR spectra were measured on Nicolet 6700 spectrometer equipped with ATR module iTR

(diamond crystal); Ge/KBr Beam splitter, DTGS receiver, and globar as radiation source were used. ^{1}H, ^{13}C{^{1}H}, and ^{19}F{^{1}H} NMR spectra were acquired on a Bruker 400 MHz Avance spectrometer (400.130 MHz for ^{1}H, 100.613 MHz for ^{13}C and 376.498 for ^{19}F) at ambient temperature. Conductivity measurements were carried out using Mettler Toledo FE30 apparatus with Inlab710 sensor for the CH_2Cl_2 solutions at RT.

Computational Details. The full geometry optimization of complexes **1**, **2**, **7**, and **8** has been carried out at the DFT level of theory using the B3LYP[76,77] and M06-2X[78] functionals with the help of *Gaussian-09*[79] program package. The standard 6-311+G** basis set was applied for all atoms. No symmetry restrictions have been applied during the geometry optimization. The Hessian matrix was calculated analytically in order to prove the location of correct minima (no imaginary frequencies). The topological analysis of the electron density distribution with help of the AIM method of Bader[80] was performed using the program AIMAll.[81] The atomic charges and bond orbital nature were analyzed by using the natural bond orbital (NBO) partitioning scheme.[82]

X-ray Structure Determinations. For single crystal X-ray diffraction experiments, crystals of **2**, **3**, **8**, **9**, **10**, **11**, **12b**, **15**, and **18** were fixed on a micro mounts, placed on a Agilent Technologies Excalibur diffractometer equipped with an Eos CCD detector and measured using monochromated Mo*Kα* radiation. Crystals of **1**, **12a**, **13**, **14**, and **16** were placed on an Agilent Technologies Supernova diffractometer equipped with an Atlas CCD detector and measured using microfocused monochromated Cu*Kα* radiation. The unit cell parameters (**Tables S2–S5**, see ESI) were refined by least square techniques. The structures have been solved by the direct methods and refined by means of the SHELXL-97 program[83] incorporated in the OLEX2 program package.[84] The carbon and nitrogen-bound H atoms were placed in calculated positions and were included in the refinement in the 'riding' model approximation, with U_{iso}(H) set to 1.5U_{eq}(C) and C–H 0.96 Å for CH_3 groups, with U_{iso}(H) set to 1.2U_{eq}(C) and C–H 0.97 Å for CH_2 groups, U_{iso}(H) set to 1.2U_{eq}(C) and C–H 0.93 Å for the CH groups, and U_{iso}(H) set to

1.2U_{eq}(N) and N–H 0.86 Å for the NH_2 groups. Positions of hydrogen atoms of mater molecules were localized objectively and kept fixed during refinement. Empirical absorption correction was applied in CrysAlisPro[85] program complex using spherical harmonics, implemented in SCALE3 ABSPACK scaling algorithm. Supplementary crystallographic data for this paper have been deposited at Cambridge Crystallographic Data Centre (**Tables S2–S5**) and can be obtained free of charge via www.ccdc.cam.ac.uk/data_request/cif.

Synthesis of [ZnX$_2$(NCNR$_2$)$_2$] (R$_2$ = Me$_2$, X = Cl **1**, X = Br **2**, X = I **3**; R$_2$ = C$_5$H$_{10}$, X = Cl **4**, X = Br **5**; X = I **6**; R$_2$ = Ph$_2$, X = Cl **7**, X = Br **8**, X = I **9**). ZnX$_2$ (1.8 mmol) was suspended in dry CH_2Cl_2 (2 mL) at RT, whereupon a solution of NCNR$_2$ (3.6 mmol) in dry dichloromethane (2 mL) was added dropwise for 5 min. The reaction mixture was stirred at RT for 2 h, whereupon a CH_2Cl_2 solution was decanted from undissolved residue of ZnX$_2$ and evaporated *in vacuo* until ½–¾ of the initial volume. Petroleum ether (40–70 °C; 2–3 mL) was added to the resulted solution and crystallization was initiated by scratching with a glass stick. Crystalline product released was separated by filtration and washed with the petroleum ether (two 5-mL portions) to give the target product as colorless hygroscopic crystals.

[ZnCl$_2$(NCNMe$_2$)$_2$] (**1**). Yield 0.408 g, 82%. Found: Zn, 23.94 (Calc. for C$_6$H$_{12}$N$_4$Cl$_2$Zn: Zn, 23.65); *m/z* (HRESI$^+$, MeOH) 309.0551 ([M – Cl + NCNMe$_2$]$^+$ requires 309.0573), 239.0029 ([M – Cl]$^+$ requires 239.0042), 168.9503 ([M – Cl – NCNC$_5$H$_{10}$]$^+$ requires 168.9511); IR v_{max}/cm^{-1} (KBr, selected bands): 2943 m (C–H), 2265 s (CN); ^{1}H NMR (acetone-d_6), δ: 2.97 (s, CH$_3$); ^{1}H NMR (DMSO-d_6), δ: 2.77 br (s, CH$_3$). ^{13}C{^{1}H} NMR (DMSO-d_6), δ 40.08 (CH$_3$), 119.46 (NCN). Crystals suitable for X-ray diffraction were obtained by a slow evaporation of an acetone/toluene (1/1, v/v) solution at RT.

[ZnBr$_2$(NCNMe$_2$)$_2$] (**2**). Yield 0.585 g, 89%. Found: Zn, 17.76 (Calc. for C$_6$H$_{12}$N$_4$Br$_2$Zn: Zn, 17.90); *m/z* (HRESI$^+$, CH$_2$Cl$_2$) 355.0025 ([M – Br + NCNMe$_2$]$^+$ requires 355.0047), 282.9532 ([M – Br]$^+$ requires 282.9537), 212.9003 ([M – Br – NCNMe$_2$]$^+$ requires 212.9006); IR v_{max}/cm^{-1} (KBr, selected bands): 2939 m (C–H), 2261 br s (CN); ^{1}H NMR (CDCl$_3$), δ: 2.99 (s, CH$_3$);

26

$^{13}C\{^1H\}$ NMR (CDCl$_3$), δ: 40.12 (CH$_3$), 119.53 (NCN). Crystals suitable for X-ray diffraction were obtained by a slow evaporation of an acetone/toluene (1/1, v/v) solution at RT.

[ZnI$_2$(NCNMe$_2$)$_2$] (**3**). Yield 0.730 g, 88%. Found: Zn, 14.58 (Calc. for C$_6$H$_{12}$N$_4$I$_2$Zn: Zn, 14.23); m/z (HRESI$^+$, CH$_2$Cl$_2$) 400.9895 ([M – I + NCNMe$_2$]$^+$ requires 400.9929, 330.9379 ([M – I]$^+$ requires 330.9398), 260.8854 ([M – I – NCNMe$_2$]$^+$ requires 260.8867); IR ν_{max}/cm^{-1} (KBr, selected bands): 2929 w (C–H), 2265 br s (CN); ^{1}H NMR (CDCl$_3$), δ: 3.01 (s, CH$_3$); $^{13}C\{^1H\}$ NMR (CDCl$_3$), δ: 40.06 (CH$_3$), 119.54 (NCN). Crystals suitable for X-ray diffraction were obtained by a slow evaporation of an acetone/toluene (1/1, v/v) solution at RT.

[ZnCl$_2$(NCNC$_5$H$_{10}$)$_2$] (**4**). Yield 0.481 g, 75%. Found: Zn, 18.09 (Calc. for C$_{12}$H$_{20}$N$_4$Cl$_2$Zn: Zn, 18.33); m/z (HRESI$^+$, MeOH) 429.1505 ([M – Cl + NCNC$_5$H$_{10}$]$^+$ requires 429.1512), 319.0669 ([M – Cl]$^+$ requires 319.0668), 208.9818 ([M – Cl – NCNC$_5$H$_{10}$]$^+$ requires 208.9824); IR ν_{max}/cm^{-1} (KBr, selected bands): 2950 m (C–H), 2258 br s, 2212 m (CN); ^{1}H NMR (CDCl$_3$), δ: 1.60 (2H, m, CH$_2$), 1.68 (4H, m, CH$_2$), 3.31 (4H, m, CH$_2$); $^{13}C\{^1H\}$ NMR (CDCl$_3$), δ: 22.59, 24.54 (CH$_2$), 49.64 (N(CH$_2$)$_2$), 118.41 (NCN).

[ZnBr$_2$(NCNC$_5$H$_{10}$)$_2$] (**5**). Yield 0.753 g, 94%. Found: Zn, 14.14 (Calc. for C$_{12}$H$_{20}$N$_4$Br$_2$Zn: Zn, 14.68); m/z (HRESI$^+$, CH$_2$Cl$_2$) 475.0996 ([M – Br + NCNC$_5$H$_{10}$]$^+$ requires 475.0986), 365.0161 ([M – Br]$^+$ requires 365.0142), 254.9290 ([M – Br – NCNC$_5$H$_{10}$]$^+$, requires 254.9298); IR ν_{max}/cm^{-1} (KBr, selected bands): 2949 m (C–H), 2257 br s (CN); ^{1}H NMR (CDCl$_3$), δ: 1.60 (2H, m, CH$_2$), 1.68 (4H, m, CH$_2$), 3.31 (4H, m, CH$_2$); $^{13}C\{^1H\}$ NMR (CDCl$_3$), δ: 22.55, 24.56 (CH$_2$), 49.72 (N(CH$_2$)$_2$), 118.55 (NCN).

[ZnI$_2$(NCNC$_5$H$_{10}$)$_2$] (**6**). Yield 0.898 g, 92%. Found: Zn, 12.06 (Calc. for C$_{12}$H$_{20}$N$_4$I$_2$Zn: Zn, 12.12); m/z (HRESI$^+$, CH$_2$Cl$_2$) 521.0859 ([M – I + NCNC$_5$H$_{10}$] requires 521.0868), 411.0029 ([M – I]$^+$ requires 411.0024); 300.9175 ([M – I – NCNC$_5$H$_{10}$]$^+$ requires 300.9180). IR ν_{max}/cm^{-1} (KBr, selected bands): 2943 s (C–H), 2258 s (CN); ^{1}H NMR (CDCl$_3$), δ: 1.59–1.65 (2H, m,

CH$_2$), 1.69–1.74 (4H, m), 3.32–3.35 (4H, m); ^{13}C{^{1}H} NMR (CDCl$_3$), δ: 22.61, 24.68 (CH$_2$), 49.69 (N(CH$_2$)$_2$), 118.90 (NCN).

[ZnCl$_2$(NCNPh$_2$)$_2$] (**7**). Yield 0.727 g, 77%. Found: Zn, 12.44 (Calc. for C$_{26}$H$_{20}$N$_4$Cl$_2$Zn: Zn, 12.46); m/z (HRESI$^+$, CH$_2$Cl$_2$) 681.1485 ([M – Cl + NCNPh$_2$]$^+$ requires 681.1512), 487.0657 ([M – Cl]$^+$ requires 487.0668); IR v_{max}/cm^{-1} (KBr, selected bands): 2264 w, 2223 s (CN); ^{1}H NMR (CDCl$_3$), δ: 7.25–7.27 (4H, m, Ph), 7.30–7.33 (2H, m, Ph), 7.42–7.46 (4H, m, Ph); ^{13}C{^{1}H} NMR (CDCl$_3$), δ: 121.91, 127.51, 130.36, 137.83 (Ph), 113.57 (NCN). Crystals for X-ray diffraction were obtained by slow evaporation of a toluene/acetone (1/1, v/v) solution at RT.

[ZnBr$_2$(NCNPh$_2$)$_2$] (**8**). Yield 0.571 g, 75% (washed with 3-mL portion of Et$_2$O). Found: Zn, 10.70 (Calc. for C$_{26}$H$_{20}$N$_4$Br$_2$Zn: Zn, 10.66); m/z (HRESI$^+$, CH$_2$Cl$_2$) 531.0046 ([M – Cl]$^+$ requires 531.0163); IR v_{max}/cm^{-1} (KBr, selected bands): 2264 w, 2226 s (CN); ^{1}H NMR (CDCl$_3$), δ: 7.25–7.27 (4H, m, Ph), 7.30–7.33 (2H, m, Ph), 7.42–7.46 (4H, m, Ph); ^{13}C{^{1}H} NMR (CDCl$_3$), δ: 121.92, 127.62, 130.39, 137.71 (Ph), 113.65 (NCN). Crystals suitable for X-ray diffraction were obtained by a slow evaporation of an acetone/toluene (1/1, v/v) solution at RT.

[ZnI$_2$(NCNPh$_2$)$_2$] (**9**) Yield 1.04 g, 82%. Found: Zn, 9.02 (Calc. for C$_{26}$H$_{20}$N$_4$I$_2$Zn: Zn, 9.24); m/z (HRESI$^+$, CH$_2$Cl$_2$) 773.0833 (M – I + NCNPh$_2$] requires 773.0868), 579.0001 ([M – I]$^+$ requires 579.0024); IR v_{max}/cm^{-1} (KBr, selected bands): 2258 m, 2226 s (CN); ^{1}H NMR (CDCl$_3$), δ: 7.26–7.30 (4H, m, Ph), 7.34–7.38 (2H, m, Ph), 7.45–7.49 (4H, m, Ph); ^{13}C{^{1}H} NMR (acetone-d_6), δ: 122.16, 127.34, 130.97, 140.14 (Ph), 113.04 (NCN).

Preparation of crystals of 10 and 11 for X-ray diffraction studies. The crystals of **10** were prepared by the slow (for 2 months) evaporation of CDCl$_3$ solution of **7** at RT from an NMR tube. The crystals of **11** were obtained by evaporation of acetone/toluene (1/1, v/v) solution of **8** at RT for 2 d. Despite amounts of **10** and **11** were small, we succeeded in their identification not only by X-ray crystallography, but also by HRESI-MS and ^{1}H NMR.

Synthesis of 11. A mixture of $ZnBr_2$ (0.161 g, 0.71 mmol) and $NCNPh_2$ (0.184 g, 0.95 mmol) in CH_2Cl_2 (2 mL) was stirred at RT for 6 d. During this time 3/4 of initial volume of the solvent evaporated and large colorless crystals formed. The crystals were filtered, washed with hexane to give 0.184 g (54%) of colorless precipitate of **11**.

[Zn(NCNPh₂)₄(H₂O)₂][Zn₂(μ-Cl)₂Cl₄] (**10**) m/z (HRESI⁺, CH_2Cl_2) 420.1346 ([M − 2H₂O − Zn_2Cl_6]²⁺ requires 420.1335); ¹H NMR (acetone-d_6), δ: 7.29–7.54 (m, Ph), 3.93 (s, H₂O).

[Zn(NCNPh₂)₄(H₂O)₂][Zn₂(μ-Br)₂Br₄] (**11**) Yield 0.184 g, 54%. Found: Zn, 13.55 (Calc. for $C_{52}H_{44}Br_6N_8O_2Zn_3$: Zn, 13.18); m/z (HRESI⁺, MeOH) 420.1328 ([M − 2H₂O − Zn_2Br_6]²⁺ requires 420.1335), (HRESI⁺, MeOH) 304.6800 ([Zn_2Br_6]²⁻ requires 304.6796); IR v_{max}/cm^{-1} (KBr, selected bands): 2223 (CN), 1600 (C-C, Ph); ¹H NMR (CDCl₃), δ: 7.24–7.46 (m, Ph), 4.05 (br, H₂O). ¹³C{¹H} NMR (CDCl₃), δ: 138.13, 130.27, 127.28, 121.77 (Ph), 113.36 (NCN).

Synthesis of [Zn(SO₃CF₃)₂(NCNR₂)₃] (**12**, **13**). *Method A.* A solution of $AgSO_3CF_3$ (1.09 mmol) in dry acetone (1 mL) was added dropwise for 2 min under argon at RT to a stirred solution of [$ZnCl_2(NCNR_2)_2$] (0.55 mmol) in dry acetone (4 mL). After 15 min, $NCNR_2$ (1.83 mmol) was added to the reaction mixture that was stirred for 2 h at RT, whereupon released AgCl was filtered off. The filtrate was concentrated under reduced pressure (*ca*. 5 mbar) giving an oily residue that was washed with petroleum ether (40–70 °C; two 2-mL portions) to give the target product as colorless hygroscopic crystalline solid. *Method B.* A solution of $NCNR_2$ (0.84 mmol) in dry CH_2Cl_2 (1 mL) was added as one portion to a suspension of zinc triflate (0.275 mmol) in dry CH_2Cl_2 (**12**, **13**) (2 mL) at RT and stirred for 2 h to give a clear colorless solution. The reaction mixture was then concentrated to dryness and oily residue thus obtained was treated with petroleum ether (40–70 °C; six 5-mL portions) and crystallized by scratching with a glass stick. Crystalline product released was separated by filtration and washed with petroleum ether (5 mL) to give the target product as colorless hygroscopic powder. Complexes **11** and **12** can be

obtained similarly and in the same yields by *Method B* starting from **4**, **5**, **7**, and **8**, correspondingly.

[Zn(SO₃CF₃)₂(NCNMe₂)₃] (**12**). Method A. Yield 0.119 g, 76%. Method B. Yield 0.131 g, 83%. Found: Zn, 11.53 (Calc. for $C_{11}H_{18}N_6S_2O_6F_6Zn$: Zn, 11.40); *m/z* (HRESI⁺, MeOH) 423.0440 ([M– CF₃SO₃]⁺ requires 423.0405); IR v_{max}/cm⁻¹ (KBr, selected bands): 2940 m (C–H), 2265 br, s (C≡N) and 2220 narrow, s (C≡N) (free NCNMe₂). ATR v_{max}/cm⁻¹ (selected bands): 2952 s (C–H), 2251 br, s. ¹H NMR (CDCl₃), δ: 2.89 (s, CH₃); ¹³C{¹H} NMR (DMSO-d_6), δ: 40.12 (CH₃), 115.99, 119.19, 122.40 (CF₃), 119.53 (CN). ¹³C{¹H} NMR (acetone-d_6), δ: 40.30 (CH₃), 116.66, 119.84, 123.01, 126.22 (CF₃), 120.32 (CN). ¹³C{¹H} NMR (CDCl₃), δ: 40.41 (CH₃), 119.44 (NCN); ¹⁹F{¹H} NMR (acetone-d_6), δ: −79.05 (CF₃SO₃). When complex **12** (prepared by method A) was crystallized in an open beaker without solvent, we obtained crystals of **12a**. When **12** (prepared by method B) was dissolved in dry CH₂Cl₂, the obtained solution was kept in a closed flask for 1d, whereupon the solvent was rapidly evaporated to give crystals of **12b**. Both **12a** and **12b** were studied by X-ray crystallography.

[Zn(SO₃CF₃)₂(NCNC₅H₁₀)₃] (**13**). Method A. Yield 0.125 g, 79%. Method B. Yield 0.162 g, 85%. Found: Zn, 9.53 (Calc. for $C_{20}H_{30}N_6S_2O_6F_6Zn$: Zn, 9.42); *m/z* (HRESI⁺, MeOH) 543.1335 ([M − SO₃CF₃]⁺ requires 543.1344); IR v_{max}/cm⁻¹ (KBr, selected bands): 2950 br, m (CH) , 2242 s, 2231 m (CN); ATR v_{max}/cm⁻¹ (selected bands): 2952 s (CH), 2251 br, s (CN); ¹H NMR (acetone-d_6), δ: 1.64 (2H, m, CH₂), 1.68 (4H, m, CH₂), 3.34 (4H, m, CH₂); ¹³C{¹H} NMR (CDCl₃), δ: 22.36, 25.29 (CH₂), 50.47 (N(CH₂)₂), 119.56 (NCN), 119.71, 122.88, 126.06 (CF₃); ¹⁹F{¹H} NMR (acetone-d_6), δ: −79.01 (CF₃SO₃).

Zn-mediated hydration of dialkylcyanamide ligands. Generation of [ZnX₂{OC(NH₂)NR₂}₂] (X = Cl, Br, I; R₂ = Me₂, C₅H₁₀; 14–19). Suspension of ZnX₂ (0.80 mmol), NCNR₂ (1.60 mmol), and water (0.6 mL, 33 mmol) in acetone (4 mL) was heated at 60 °C in a screw-cap closed vial for 3 d. During this time the reaction mixture was partially

evaporated until *ca.* ¼ of the initial volume. Resulted viscous mixture was cooled to RT to give

crystals that were studied by X-ray diffraction. Reaction mixture was dissolved in acetone,

filtered, and the filtrate was evaporated. Viscous residue formed was treated with hexane (three

20-mL portions; with evaporation to dryness every time) to give the title product as a beige

powder. The powder was treated with a mixture of hexane/acetone (8/2, v/v; three 5-mL

portions) to remove admixture of the starting complex and this purification procedure was

monitored by IR spectroscopy and the monitoring is based upon disappearing of the v(CN) band.

[ZnCl$_2${OC(NH$_2$)NMe$_2$}$_2$] (**14**). Yield 0.250 g, 60%. Found: Zn, 20.80 (Calc. for C$_6$H$_{16}$-
N$_4$Cl$_2$O$_2$Zn: Zn, 20.92) m/z (HRESI$^+$, MeOH) 275.0248 ([M – Cl]$^+$ requires 275.0253); IR
v_{max}/cm^{-1} (KBr, selected bands): 3448, 3356 s, br, 1600 s (NH$_2$), 2937 w (C–H), 1657, 1633 s, br
(C=O). ^{1}H NMR (DMSO-d_6), δ: 2.75 (s, CH$_3$), 5.77 (s, br, NH$_2$); ^{13}C{^{1}H} NMR (DMSO-d_6), δ:
35.95 (Me), 159.14 (C=O). Crystals suitable for X-ray diffraction were obtained directly from
the reaction mixture. Crystal structure of this complex is known[57,58] (our data: space group *Pbca*,
a =18.5884(11), b = 13.2455(7), c = 10.3779(9) Å, V = 2555.2(3) Å^3; *lit.*[58] D_{2h}(15) – *Pbca*, a =
18.77(5), b = 13.74(2), c = 10.50(1) Å, V = not reported).

[ZnBr$_2${OC(NH$_2$)NMe$_2$}$_2$] (**15**). Yield 0.255 g, 80%. Found: Zn, 16.18 (Calc. for
C$_6$H$_{16}$N$_4$Br$_2$O$_2$Zn: Zn, 16.29); m/z (HRESI$^+$, MeOH) 320.9697 ([M – Br]$^+$ requires 320.9728); IR
v_{max}/cm^{-1} (KBr, selected bands): 3450, 3358 s, br, 1600 s (NH$_2$), 2940 s (C–H), 1655, 1633 s, br
(C=O); ^{1}H NMR (DMSO-d_6), δ: 2.75 (s, CH$_3$), 5.75 (s, br, NH$_2$); ^{13}C{^{1}H} NMR (DMSO-d_6), δ:
35.95 (Me), 159.11 (C=O). Crystals suitable for X-ray diffraction were obtained directly from
the reaction mixture. Crystal structure of this complex is known[57,58] (our data: space group *P*
2$_1$/n, a = 14.1711(8), b = 12.6536(9), c = 7.5270(5) Å, $β$ = 89.364(6), V = 1349.62 Å^3; *lit.*[58]
C_{2h}(5)–*P*2$_1$/c, a = 16.17(9), b = 12.70(2) Å, c = 7.62(1) Å, $β$ = 117.3, V = 1390 Å^3).

 [ZnI$_2${OC(NH$_2$)NMe$_2$}$_2$] (**16**). Yield 0.297 g, 76%. Found: Zn, 13.38, (Calc. for
C$_6$H$_{16}$N$_4$I$_2$O$_2$Zn: Zn, 13.20); m/z (HRESI$^+$, MeOH) 366.9530 ([M – I]$^+$ requires 366.9604); IR
v_{max}/cm^{-1} (KBr, selected bands): 3450, 3358 s, br, 1600 s (NH$_2$), 2933 w (C–H), 1651, 1626 s, br

(C=O); ^{1}H NMR (DMSO-d_6), δ: 2.74 (s, CH$_3$), 5.75 (s, br, NH$_2$); ^{13}C{^{1}H} NMR (DMSO-d_6), δ: 35.97 (Me), 159.09 (C=O).

[ZnCl$_2${OC(NH$_2$)NC$_5$H$_{10}$}$_2$] (**17**). Yield 0.246g, 78%. Found: Zn, 17.10, (Calc. for C$_{12}$H$_{24}$N$_4$Cl$_2$O$_2$Zn: Zn, 16.66); m/z (HRESI$^+$, MeOH) 355.0892 ([M – Cl]$^+$ requires 355.0879); IR v_{max}/cm^{-1} (KBr, selected bands): 3433, 3343 s, br, 1580 s (NH$_2$), 2944 s (C–H), 1658, 1637, br (C=O); ^{1}H NMR (DMSO-d_6), δ: 1.38 (m, CH$_2$), 1.50 (m, CH$_2$), 3.22 (m, CH$_2$), 5.85 (s, br, NH$_2$); ^{13}C{^{1}H} NMR (DMSO-d_6), δ: 24.11, 25.43, 44.32 (piperidine), 158.09 (C=O). Crystals suitable for X-ray diffraction were obtained directly from the reaction mixture.

[ZnBr$_2${OC(NH$_2$)NC$_5$H$_{10}$}$_2$] (**18**). Yield 0.312 g, 81%. Found: Zn, 14.24 (Calc. for C$_{12}$H$_{24}$N$_4$Br$_2$O$_2$Zn: Zn, 13.58); m/z (HRESI$^+$, MeOH) 401.0337 ([M – Br]$^+$ requires 401.0354); IR v_{max}/cm^{-1} (KBr, selected bands): 3443, 3354 s, br, 1580 s (NH$_2$), 2944 s (C–H), 1648, 1630 s, br (C=O); ^{1}H NMR (DMSO-d_6), δ: 1.38 (m, CH$_2$), 1.49 (m, CH$_2$), 3.32 (m, CH$_2$), 5.81 (s, br, NH$_2$); ^{13}C{^{1}H} NMR (DMSO-d_6), δ: 24.10, 25.41, 44.30 (piperidine), 158.02 (C=O); ^{13}C{^{1}H} NMR (CD$_3$OD), δ: 25.34, 26.75, 45.03 (piperidine), 161.13 (C=O). Crystals suitable for X-ray diffraction were obtained directly from the reaction mixture.

[ZnI$_2${OC(NH$_2$)NC$_5$H$_{10}$}$_2$] (**19**). Yield 0.368 g, 80%. Found: Zn, 11.02, (Calc. for C$_{12}$H$_{24}$N$_4$I$_2$O$_2$Zn: Zn, 11.36); m/z (HRESI$^+$, MeOH) 447.0234 ([M – I]$^+$ requires 447.0235); IR v_{max}/cm^{-1} (KBr, selected bands): 3440, 3370 sh, s, br, 1580 s (NH$_2$), 2940 s (C–H), 1637 s (C=O); ^{1}H NMR (DMSO-d_6), δ: 1.38 (m, CH$_2$), 1.51 (m, CH$_2$), 3.32 (m, CH$_2$), 5.82 (s, br, NH$_2$); ^{13}C{^{1}H} NMR (DMSO-d_6), δ: 24.08, 25.40, 44.29 (piperidine), 158.00 (C=O).

Reaction of [ZnX$_2$(NCNPh$_2$)$_2$] (X = Cl, Br, I) with H$_2$O. Identification of [ZnX$_2${OC(NH$_2$)NPh$_2$}$_2$] (20–22) and OC(NH$_2$)NPh$_2$. Suspension of ZnX$_2$ (1.5 mmol), diphenylcyanamide (0.596 g, 3.07 mmol), and water (0.50 mL, 28 mmol) in acetone (4 mL) was heated at 80 °C in a screw-cap closed vial for 24 h. During this time the reaction mixture was evaporated until ¼ of the initial volume. Viscous residue was dissolved in acetone, loaded on silica (1 g; Merck, 0.063-0.200 mm) and then purified by column chromatography (column: d =

15 mm, l = 55 mm), EtOAc/hexane mixture (1/1, v/v) was used as eluent with a gradient to neat

EtOAc. Finally colorless oily residue was isolated that was crystallized upon drying *in vacuo*.

This solid, based on IR, HRESI-MS and Zn analysis data, contains a mixture of the complex

$[ZnCl_2\{OC(NH_2)NPh_2\}_2]$ and the urea. Complex $[ZnI_2\{OC(NH_2)NPh_2\}_2]$ decomposed on SiO_2

column, and it was not liberated, but identified in the reaction mixture.

$[ZnCl_2\{OC(NH_2)NPh_2\}_2]$ (**20**). Yield 0.418 g, 57%. *m/z* (HRESI[+], MeOH) 523.0835 ([M – Cl][+]

requires 523.0879); IR ν_{max}/cm^{-1} (KBr, selected bands): 3475, 3330 s, br, 1590 m (NH$_2$), 1637 s,

br (C=O). ^{1}H NMR (DMSO-d_6), δ: 7.17–7.37 (m, Ph) 5.90 (s, br, NH$_2$); ^{13}C{^{1}H} NMR (DMSO-

d_6), δ: 125.64, 127.40, 129.08, 143.49 156.44. This complex contains an admixture of

OC(NH$_2$)NPh$_2$ (*ca*. 6:1 mol/mol as estimated by Zn analysis), which we failed to separate using

column chromatography. This admixture leads to unsatisfactory Zn analysis and therefore it is

not reported.

$[ZnBr_2\{OC(NH_2)NPh_2\}_2]$ (**21**). Yield 0.500 g, 69%. Found: Zn, 10.51 (Calc. for

$C_{26}H_{24}N_4Br_2O_2Zn$: Zn, 10.07); *m/z* (HRESI[+], MeOH) 569.0401 ([M – Br][+] requires 569.0354);

IR ν_{max}/cm^{-1} (KBr, selected bands): 3482 s (NH$_2$), 1631 s, br (C=O); ^{1}H NMR (DMSO-d_6), δ:

7.17–7.36 (m, Ph) 5.90 (s, br, NH$_2$); ^{13}C{^{1}H} NMR (DMSO-d_6), δ: 125.65, 127.40, 129.08,

143.48 156.44.

$[ZnI_2\{OC(NH_2)NPh_2\}_2]$ (**22**). Yield 0.300 g, 27%. *m/z* (HRESI[+], MeOH) 615.0238 ([M – I][+]

requires 615.0235); IR ν_{max}/cm^{-1} (KBr, selected bands): 3454 s, br (NH$_2$), 1633 s, br (C=O). ^{1}H

NMR DMSO-d_6), δ: 7.17–7.35 (m, Ph) 5.87 (s, br, NH$_2$)

the contract within the "FCT Investigator" program. Physicochemical studies were performed at Center for Magnetic Resonance, Center for X-ray Diffraction Studies, and Center for Chemical Analysis and Materials Research, and "Geomodel" Center (Saint Petersburg State University).

References

1.   V. Y. Kukushkin and A. J. L. Pombeiro, *Chem. Rev.*, 2002, **102**, 1771–1802.

2.   V. Y. Kukushkin and A. J. L. Pombeiro, *Inorg. Chim. Acta*, 2005, **358**, 1–21.

3.   N. A. Bokach, M. L. Kuznetsov, and V. Y. Kukushkin, *Coord. Chem. Rev.*, 2011, **255**, 2946–2967.

4.   T. J. Ahmed, S. M. M. Knapp, and D. R. Tyler, *Coord. Chem. Rev.*, 2011, **255**, 949–974.

5.   M. Kobayashi and S. Shimizu, *Curr. Opin. Chem. Biol.*, 2000, **4**, 95–102.

6.   R. A. Michelin, P. Sgarbossa, S. Mazzega Sbovata, V. Gandin, C. Marzano, and R. Bertani, *ChemMedChem*, 2011, **6**, 1172–1183.

7.   S.-I. Murahashi and H. Takaya, *Acc. Chem. Res.*, 2000, **33**, 225–233.

8.   N. A. Bokach, *Russ. Chem. Rev.*, 2010, **79**, 89–100.

9.   J. L. Eglin, *Comments Inorg. Chem.*, 2002, **23**, 23–43.

10.   B. Neumueller, *Z. Anorg. Allg. Chem.*, 2007, **633**, 193–204.

11.   A. J. L. Pombeiro and V. Y. Kukushkin, in *Compr. Coord. Chem. II*, Elsevier Ltd., 2004, vol. 1, pp. 639–660.

12.   N. A. Bokach and V. Y. Kukushkin, *Coord. Chem. Rev.*, 2013, **257**, 2293–2316.

13.   T. B. Anisimova, N. A. Bokach, K. V Luzyanin, M. Haukka, and V. Y. Kukushkin, *Dalton Trans.*, 2010, **39**, 10790–8.

14.   T. B. Anisimova, N. A. Bokach, F. M. Dolgushin, and V. Y. Kukushkin, *Dalt. Trans.*, 2013, **42**, 12460–12467.

15.   A. S. Kritchenkov, N. A. Bokach, M. Haukka, and V. Y. Kukushkin, *Dalt. Trans.*, 2011, **40**, 4175–4182.

16.   A. S. Kritchenkov, N. A. Bokach, M. L. Kuznetsov, F. M. Dolgushin, T. Q. Tung, A. P. Molchanov, and V. Y. Kukushkin, *Organometallics*, 2012, **31**, 687–699.

17.   A. S. Kritchenkov, N. A. Bokach, G. L. Starova, and V. Y. Kukushkin, *Inorg. Chem.*, 2012, **51**, 11971–11979.

18.   D. S. Bolotin, N. A. Bokach, M. Haukka, and V. Y. Kukushkin, *ChemPlusChem*, 2012, **77**, 31–40.

19.   D. S. Bolotin, N. A. Bokach, M. Haukka, and V. Y. Kukushkin, *Inorg. Chem.*, 2012, **51**, 5950–5964.
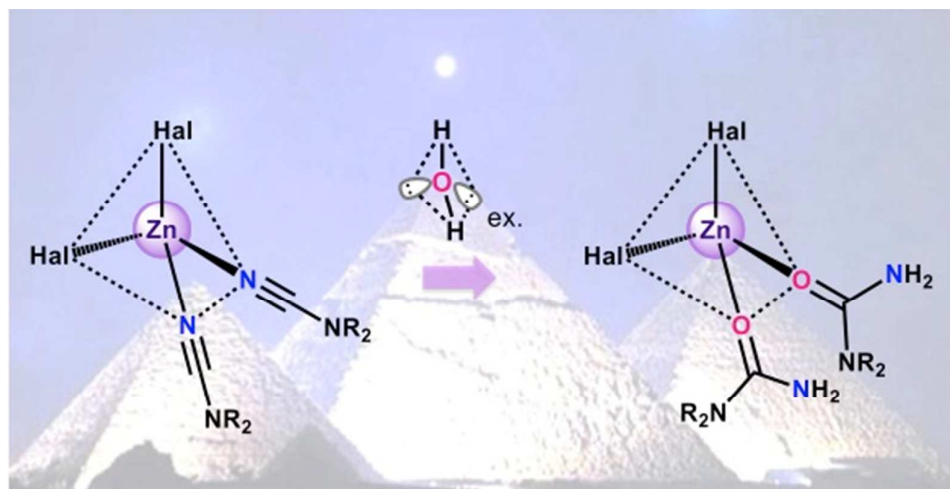
20. D. S. Bolotin, N. A. Bokach, A. S. Kritchenkov, M. Haukka, and V. Y. Kukushkin, *Inorg. Chem.*, 2013, **52**, 6378–6389.

21. J. C. Jochims, R. Abu-El-Halawa, L. Zsolnai, and G. Huttner, *Chem. Ber.*, 1984, **117**, 1161–1177.

22. T. Kamo and M. Kimura, Bull. Chem. Soc. Jpn., 1972, **45**, 3309–3314.

23. S. F. Sousa, E. S. Carvalho, D.M. Ferreira, I. S. Tavares, P.A. Fernandes, M. J. Ramos, and J. A. N. F. Gomes, *J. Comput. Chem.*, 2009, **30**, 2752–2763.

24. E. N. Yurchenko, E. B. Burgina, and L. V. Konovalov, *Zh. Struct. Khim.*, 1981, **22**, 81–87; *Chem. Abs*. 1982:517592.

25. E. N. Yurchenko, E. T. Devyatkina, and E. B. Burgina, *Zh. Strukt. Khim.*, 1977, **18**, 189–193; *Chem. Abs*. 1978:41926.

26. Y. Hase, C. Airoldi, Y. Gushikem, and Y. Kawano, *Spectrosc. Lett.*, 1976, **9**, 105–112.

27. F. Braggio, *Atti della Accad. Naz. dei Lincei, Cl. di Sci. Fis. Mat. e Nat. Rend.*, 1968, **44**, 779–782; *Chem. Abs*. 1969:453964.

28. W. Libus, D. Puchalska, and T. Szuchnicka, *J. Phys. Chem.*, 1967, **7**, 2075–2080.

29. J. C. Evans, *Spectrochim. Acta*, 1964, **21**.

30. E. N. Zilberman and N. A. Rybakova, *Zh. Obs. Khim.*, 1962, **32**, 591–596; *Chem. Abs*. 1963:33026.

31. I. V. Isakov and Z. V. Zvonkova, *Dokl. Akad. Nauk SSSR*, 1962, **145**, 801–803; *Chem. Abs*. 1962:473092.

32. R. J. Crutchley, *Coord. Chem. Rev.*, 2001, **219**–**221**, 125–155.

33. H. Fischer and R. Maerkl, *Chem. Ber.*, 1985, **118**, 3683–3699.

34. G. Bhosekar, I. Jess, and C. Naether, *Z. Naturforsch., B Chem. Sci.*, 2006, **61**, 721–726.

35. G. Bhosekar, I. Jess, and C. Naether, *Acta Crystallogr. Sect. E Struct. Reports Online*, 2006, **62**, m1315–m1316.

36. I. Rozas, I. Alkorta, and J. Elguero, *J. Am. Chem. Soc.*, 2000, **122**, 11154–11161.

37. F. Basolo, *Coord. Chem. Rev.*, 1968, **3**, 213–223.

38. A. D. Julian, C. M.Hockensmith, V. Y. Kukushkin, and Y. N. Kukushkin, in *Synthetic Coordination Chemistry: Principles and Practice*, 1997, pp. 35–57.

39. B.-H. Ye, F. Xue, G.-Q. Xue, L.-N. Ji, and T. C. W. Mak, *Polyhedron*, 1999, **18**, 1785–1790.

40.   J.-H. Deng, G.-Q. Guo, and D.-C. Zhong, *Acta Crystallogr. Sect. E Struct. Reports Online*, 2007, **63**, m2696–m2697, Sm2696/1–Sm2696/7.

41.   L.-S. Long, X.-M. Chen, and L.-N. Ji, *Inorg. Chem. Commun.*, 1999, **2**, 181–183.

42.   W. Starosta and J. Leciejewicz, *Acta Crystallogr. Sect. E Struct. Reports Online*, 2009, **65**, m640.

43.   B. Mueller and H. Vahrenkamp, *Eur. J. Inorg. Chem.*, 1999, 117–127.

44.   V. K. Bel'sky, N. R. Streltsova, B. M. Bulychev, L. V Ivankina, A. I. Gorbunov, and P. A. Storozhenko, *Inorg. Chim. Acta*, 1989, **164**, 211–220.

45.   D.-Z. Li, Y. Wang, W.-X. Zhang, S.-G. Zhang, J. Guang, and Z.-F. Xi, *Organometallics*, 2011, **30**, 5278–5283.

46.   D. Li, J. Guang, W.-X. Zhang, Y. Wang, and Z. Xi, *Org. Biomol. Chem.*, 2010, **8**, 1816–1820.

47.   B. J. Duncombe, L. Puskar, B. Wu, and A. J. Stace, *Can. J. Chem*, 2005, **83**, 1994–2005.

48.   R. Garcia-Alvarez, P. Crochet, and V. Cadierno, *Green Chem.*, 2013, **15**, 46–66.

49.   M. N. Kopylovich, V. Y. Kukushkin, M. Haukka, J. J. R. Fraústo da Silva, and A. J. L. Pombeiro, *Inorg. Chem.*, 2002, **41**, 4798–804.

50.   C. Battilocchio, J. M. Hawkins, and S. V Ley, *Org. Lett.*, 2014, **16**, 1060–1063.

51.   U. B. Patil, A. S. Singh, and J. M. Nagarkar, *RSC Advances*, 2014, **4**, 1102–1106.

52.   X. Ma, Y. He, P. Wang, and M. Lu, *Appl. Organomet. Chem.*, 2012, **26**, 377–382.

53.   A. J. L. Pombeiro, V. Yu. Kukushkin, M. N. Kopylovich, and J. J. R. Frausto da Silva, *PCT Int. Appl.*, 2002, 17 pp.; *Chem. Abs*. 2002:927387.

54.   X. Ma, Y. He, P. Wang, and M. Lu, *Appl. Organomet. Chem.*, 2012, **26**, 377–382.

55.   K. Manjula and M. A. Pasha, *Synth. Commun.*, 2007, **37**, 1545–1550.

56.   Z. S. Muksumova, N. O. Orozbaeva, Y. D. Fridman, A. K. Molodkin, and K. Rysmendeev, *Zh. Neorg. Khim.*, 1986, **31**, 2865–2869; *Chem. Abs*. 1987:77631.

57.   L. Coghi and M. Cingi, *Ateneo Parm.*, 1960, **31**, 132–138; *Chem. Abs*. 1962:1035.

58.   M. Biagini Cingi, L. Coghi, and C. Guastini, *Gazz. Chim. Ital.*, 1965, **95**, 368–374.

59.   N. G. Furmanova, V. F. Resnyanskii, K. S. Sulaimankulov, D. K. Sulaimankulova, and S. Z. Zhorobekova, *Kristallografiya*, 1998, **43**, 269–271; *Chem. Abs*. 1998:237666.

60.   H. M. K. K. Pathirana, T. J. Weiss, J. H. Reibenspies, R. A. Zingaro, and E. A. Meyers, *Z. Krist.*, 1994, **209**, 696.

61. N. A. Bokach, T. B. Pakhomova, V. Y. Kukushkin, M. Haukka, and A. J. L. Pombeiro, *Inorg. Chem.*, 2003, **42**, 7560–7568.

62. K. V Luzyanin, M. Haukka, N. A. Bokach, M. L. Kuznetsov, V. Y. Kukushkin, and A. J. L. Pombeiro, *J. Chem. Soc. Dalton Trans.*, 2002, 1882–1887.

63. P. Maslak, J. J. Sczepanski, and M. Parvez, *J. Am. Chem. Soc.*, 1991, **113**, 1062–1063.

64. D. P. Fairlie, T. C. Woon, W. A. Wickramasinghe, and A. C. Willis, *Inorg. Chem.*, 1994, **33**, 6425–6428.

65. Y. E. Ibragimova, O. F. Khodzhaev, and N. A. Parpiev, *Russ. J. Gen. Chem.*, 2013, **83**, 1419–1423.

66. T. B. Anisimova, N. A. Bokach, F. M. Dolgushin, and V. Y. Kukushkin, *Dalton Trans.*, 2013, **42**, 12460–12467.

67. C. Cannon and A. Apblett, in *Abstracts of Papers, 245th ACS National Meeting & Exposition, New Orleans, LA, United States, April 7-11, 2013*, American Chemical Society, 2013, p. INOR–1385; *Chem. Abs.* 2013:481332.

68. G. Travagli, *Gazz. Chim. Ital.*, 1957, **87**, 673–681.

69. D. P. Fairlie, W. G. Jackson, B. W. Skelton, H. Wen, A. H. White, W. A. Wickramasinghe, T. C. Woon, and H. Taube, *Inorg. Chem.*, 1997, **36**, 1020–1028.

70. N. E. Dixon, D. P. Fairlie, W. G. Jackson, and A. M. Sargeson, *Inorg. Chem.*, 1983, **22**, 4038–4046.

71. Z. Zhang, Y. He, Q. Zhao, W. Xu, Y.-Z. Li, and Z.-L. Wang, *Inorg. Chem. Commun.*, 2006, **9**, 269–272.

72. R. T. Hamilton and J. A. V. Butler, *J. Chem. Soc*, 1932, 2282–2284.

73. Y. Murakami, Y. Yokoyama, C. Sasakura, and M. Tawagawa, *Chem. Pharm. Bull.*, 1983, **31**, 423–428.

74. F. Kurzer, *J. Chem. Soc*, 1949, 3033–3038.

75. G. Schwarzenbach and H. Flaschka, *Die Komplexometrische Titration (Die Chemische Analyse, Band 45) (Complexometric Titration (Chemical Analysis, Vol. 45)). 5th ed.*, Enke, 1965.

76. A. D. Becke, *J. Chem. Phys.*, 1993, **98**, 5648–5652.

77. C. Lee, W. Yang, and R. G. Parr, *Phys. Rev. B Condens. Matter Mater. Phys.*, 1988, **37**, 785–789.

78. Y. Zhao and D. G. Truhlar, *Theor. Chem. Acc.*, 2008, **120**, 215–241.

79. M. J. Frisch, G. W. Trucks, H. B. Schlegel, G. E. Scuseria, M. A. Robb, J. R. Cheeseman, G. Scalmani, V. Barone, B. Mennucci, G. A. Petersson, H. Nakatsuji, M. Caricato, X. Li, H. P. Hratchian, A. F. Izmaylov, J. Bloino, G. Zheng, J. L. Sonnenberg, M. Hada, K. Ehara, K. Toyota, R. Fukuda, J. Hasegawa, M. Ishida, T. Nakajima, Y. Honda, O. Kitao, H. Nakai, T. Vreven, J. A. Montgomery, J. E. J. Peralta, F. Ogliaro, M. Bearpark, J. J. Heyd, E. Brothers, K. N. Kudin, V. N. Staroverov, R. Kobayashi, J. Normand, K. Raghavachari, A. Rendell, J. C. Burant, S. S. Iyengar, J. Tomasi, M. Cossi, N. Rega, J. M. Millam, M. Klene, E. Knox, J. B. Cross, V. Bakken, C. Adamo, J. Jaramillo, R. Gomperts, R. E. Stratmann, O. Yazyev, A. J. Austin, R. Cammi, C. Pomelli, J. W. Ochterski, R. L. Martin, K. Morokuma, V. G. Zakrzewski, G. A. Voth, P. Salvador, J. J. Dannenberg, S. Dapprich, A. D. Daniels, Ö. Farkas, J. B. Foresman, J. V. Ortiz, J. Cioslowski, and D. J. Fox, *Gaussian 09*.

80. R. F. W. Bader, *Atoms in Molecules: A Quantum Theory*, Oxford University Press, Oxford, 1990.

81. Todd A. Keith, AIMAll (Version 13.01.27), TK Gristmill Software, Overland Park KS, 2013 (aim.tkgristmill.com).

82. A. E. Reed, L. A. Curtiss, and F. Weinhold, *Chem. Rev.*, 1988, **88**, 899–926.

83. G. M. Sheldrick, *Acta Crystallogr. Sect. A Found. Crystallogr.*, 2008, **64**, 112–122.

84. O. V Dolomanov, L. J. Bourhis, R. J. Gildea, J. A. K. Howard, and H. Puschmann, *J. Appl. Crystallogr.*, 2009, **42**, 339–341.

85. *CrysAlisPro, Aglient Technologies, version 1.171.36.20*, Aglient Technologies.

Graphical Abstract

The Zn^{II}-mediated hydration of cyanamides does not require any co-catalyst.